Simulation of Journal Bearings in Single cylinder Four-Stroke IC Engine: A Numerical Approach

THESIS SUBMITTED IN PARTIAL FULFILMENTS OF THE REQUIREMENT FOR THE DEGREE OF MASTER OF ENGINEERING IN AUTOMOBILE ENGINEERING UNDER FACULTY OF ENGINEERING AND TECHNOLOGY

Submitted by

ANUJ SHAW

Class Roll Number: 002211204004

Registration Number: 163718 of 2022-23

Examination Roll Number: M4AUT24003

Academic Session: 2022-2024

Under the guidance of

PROF. DR. SUSENJIT SARKAR

Department of Mechanical Engineering

Jadavpur University

188, Raja S.C. Mullick Road,

Kolkata – 700032

DECLARATION OF ORIGINALITY AND COMPLIANCE OF ACADEMIC ETHICS

I hereby declare that the thesis entitled "**SIMULATION OF JOURNAL BEARINGS IN SINGLE CYLINDER FOUR-STROKE IC ENGINE: A NUMERICAL APPROACH**" contains literature survey and original research work by the undersigned candidate, as a part of his *MASTER OF ENGINEERING IN AUTOMOBILE ENGINEERING* under the *DEPARTMENT OF MECHANICAL ENGINNERING*, studies during academic session *2022-2024.*

All information in this document have been obtained and presented in accordance with the academic rules and ethical conduct.

I also declare that, as required by these rules of conduct, I have fully cited and referenced all the material and results that are not original to this work.

Name: **ANUJ SHAW**

Class Roll Number: **002211204004**

Registration Number: **163718 of 2022-23**

Examination Roll Number: **M4AUT24003**

Date:

Signature of Candidate

FACULTY OF ENGINEERING & TECHNOLOGY

DEPARTMENT OF MECHANICAL ENGINEERING

JADAVPUR UNIVERSITY

KOLKATA

CERTIFICATE OF RECOMMENDATION

This is to certify that the thesis entitled "**Simulation of Journal Bearings in Single cylinder Four-Stroke IC Engine: A Numerical Approach**" is a bonafide work carried out by **ANUJ SHAW** under our supervision and guidance in partial fulfilment of the requirements for awarding the degree of Master of Engineering in Automobile Engineering under Department of Mechanical Engineering, Jadavpur University during the academic session 2022-2024.

Prof. Dr. Susenjit Sarkar

THESIS SUPERVISOR
Department of Mechanical Engineering
Jadavpur University, Kolkata

Prof. Dipak Laha

Dean
Faculty of Engineering and Technology
Jadavpur University, Kolkata

Prof. Dr. Swarnendu Sen

Head of the Department
Department of Mechanical Engineering
Jadavpur University, Kolkata

FACULTY OF ENGINEERING & TECHNOLOGY

DEPARTMENT OF MECHANICAL ENGINEERING

JADAVPUR UNIVERSITY

KOLKATA

CERTIFICATE OF APPROVAL

The foregoing thesis, entitled "**Simulation of Journal Bearings in Single cylinder Four-Stroke IC Engine: A Numerical Approach**" is hereby approved as a creditable study in the area of Automobile Engineering carried out and presented by **ANUJ SHAW** in a satisfactory manner to warrant its acceptance as a prerequisite to the degree for which it has been submitted. It is notified to be understood that by this approval, the undersigned do not necessarily endorse or approve any statement made, opinion expressed and conclusion drawn therein but approve the thesis only for the purpose for which it has been submitted.

Committee of final evaluation of thesis:

_____

_____

_____

ACKNOWLEDGEMENT

I am very thankful to my respected thesis supervisor **PROF. DR. SUSENJIT SARKAR**, Professor, Department of Mechanical Engineering, Jadavpur University for his excellent and resourceful guidance, which helped me a lot in the completion of this thesis. Without their supervision and constant encouragement, it would not be possible to prepare such a thesis compactly. I do convey my best regards and gratitude to them.

The regular discussions and idea-sharing with my thesis supervisors really helped me to improve my knowledge day by day in my research related problems. They were always available for me for any query, whether it was a telephonic or a face-to-face discussion. Their appreciation and encouragement in this project work really helped me to realize my aspirations towards research work. They were the key persons in my project work and their guidance, supervision as well as providing necessary information in completing my master's thesis is immense.

I am highly indebted to all my professors, their guidance and supervision as well as for providing necessary information regarding thesis and for their support in completing my master's thesis.

I would like to thank **Mr. Mintu Karmakar**, PhD scholar, for giving me valuable suggestions and guidance.

I would like to express my gratitude towards my parents and my younger brother for their kind cooperation and encouragement which helped me in the completion of my master's thesis.

Finally, my thanks and appreciations also go to my dear friends in developing my master's project and people who have willingly helped me out with their abilities.

ANUJ SHAW

M.E ("Automobile Engineering")

2nd Year, Final Semester

Department of Mechanical Engineering

Jadavpur University, Kolkata

Table of Contents

Nomenclature

- $\boldsymbol{P_p}$ Force acting on piston top due to gas pressure (N)
- $\boldsymbol{P_q}$ Thrust on connecting rod (N)
- $\boldsymbol{P_t}$ Tangential component of force on crank pin (N)
- $\boldsymbol{P_r}$ Radial component of force on crank pin (N)
- $\boldsymbol{\phi}$ Inclination angle of connecting rod with the line of dead centers (deg)
- $\boldsymbol{\theta}$ Angle of inclination of crank with line of dead centres (deg)
- $\boldsymbol{L_C}$ Length of connecting rod (mm)
- $\boldsymbol{r_C}$ Crank length (mm)
- **D** Diameter of bearing (mm)
- **R** Radius of Bearing (mm)
- $\boldsymbol{r}$ Radius of Journal (mm)
- $\boldsymbol{c}$ Clearence = $(R - r)$ mm
- $\boldsymbol{e}$ Eccentricity (mm)
- $\boldsymbol{\varepsilon}$ Eccentricity Ratio = e/c
- $\boldsymbol{L/D}$ Bearing length to Diameter ratio
- **h** Local Fluid Film Thickness = $c(1 - \varepsilon\cos(\theta - \emptyset))$ mm
- $\boldsymbol{h_{max}}$ Maximum Fluid Film Thickness = $c(1 + \varepsilon)$ mm
- $\boldsymbol{h_0}$ Minium Fluid Film Thickness = $c(1 - \varepsilon)$ mm
- $\boldsymbol{p_0}$ Atmospheric pressure = 101325 Pa
- $\boldsymbol{\mu}$ Dynamic viscosity of the fluid (Pa.s)
- $\boldsymbol{p}$ Differential local fluid film pressure (Pa)
- $\boldsymbol{U}$ Linear velocity of journal (mm/s)
- $\boldsymbol{s}$ Circumferential direction
- $\boldsymbol{z}$ Longitudinal direction
- $\emptyset$ Phase angle between Journal or crankshaft center and bearing center (deg)

- $\boldsymbol{H}$ Dimensionless flim thickness
- $\boldsymbol{\bar{P}}$ Dimensionless pressure
- $\boldsymbol{\omega}$ Angular velocity of journal or crank shaft (rad/s)
- $\boldsymbol{\Delta S}$ Dimensionless Grid spacing for pressure

List of figures

Figure Title **Page no.**

List of Tables

Table Title **Page no.**

Chapter 1

INTRODUCTION

1.1 Background

Journal bearings are vital components in rotating machinery, such as four-stroke engines, where they play a crucial role in supporting radial loads and ensuring smooth rotational motion. These bearings are designed to accommodate the shaft (or journal) and the bearing sleeve, with a thin film of lubricant acting as a critical intermediary. This lubricant film is essential as it separates the rotating shaft from the stationary bearing sleeve, minimizing direct metal-to-metal contact. By doing so, it significantly reduces friction and wear, which is crucial for maintaining the longevity and reliability of both the bearing and the overall machinery.

The performance of journal bearings is highly dependent on the effective formation and maintenance of this lubricant film. When functioning optimally, the lubricant film forms a hydrodynamic wedge that supports the radial load of the shaft, distributing forces evenly and reducing the risk of overheating and mechanical failure. Understanding the behavior of journal bearings and their lubricant films is therefore critical in engineering.

Internal combustion engines play a pivotal role in various industries, powering a wide array of vehicles and machinery. Understanding the dynamic behavior of engine components is crucial for optimizing performance, reliability, and efficiency. These engines operate on the principle of converting chemical energy from fuel into mechanical work, utilizing a cycle consisting of intake, compression, power, and exhaust strokes. In a four-stroke engine, the crankshaft plays a crucial role, converting the linear motion of the piston into rotational motion. This rotational motion is then transferred to the flywheel, which helps to smooth out the pulsations of the engine power stroke and maintain a consistent rotational speed. Among these components, bearings serve as critical elements that support rotating shafts, transmitting loads and facilitating smooth operation. The behavior of bearings is particularly influenced by the forces exerted on them, notably by the reciprocating motion of the piston in a piston-cylinder arrangement.

Journal bearings, which support the crankshaft in these engines, are critical for efficient and reliable engine performance. Understanding the pressure distribution and load capacity of these bearings is essential to enhancing engine durability and efficiency. This literature review explores the current state of research in the numerical simulation and optimization of journal bearing performance, with a focus on finite difference methods (FDM) and eccentricity optimization.

1.2 Objective of the Study

The primary objective of this study is to develop a numerical method, using the relaxation method of FDM, to simulate the pressure distribution after finding bearing reactions in a four-stroke single-cylinder IC engine using analytical method. These methods will be used to

optimize the eccentricity of journal bearings, thereby enhancing the engine's performance. The study also aims to consider various assumptions to simplify the analysis without significantly compromising the accuracy of the results.

This research focuses on investigating the dynamic characteristics of a Single Cylinder Four-Stroke Engine model, with specific emphasis on the interaction between piston motions, pressure distribution, and bearing reaction forces. The study aims to analyse these interactions throughout a complete engine cycle by assuming linear characteristics of piston pressure for different crank angle positions.

By understanding the forces experienced by bearings and accurately predicting journal positions, the study seeks to provide practical implications for enhancing engine performance and durability.

1.3 Significance of the Research

Accurate pressure distribution analysis in IC engines is crucial for optimizing bearing performance, reducing wear, and improving overall engine efficiency.

Researchers focus on optimizing these bearings to improve their performance, which involves studying factors such as pressure distribution analysis, wear analysis, lubricant viscosity, bearing geometry, and load conditions. Advances in this field contribute to more durable and efficient engines, making the study of journal bearings a key area of interest for enhancing the design and operation of modern machinery.

This research contributes to the field by providing a detailed numerical approach for pressure distribution simulation and optimization, applicable to various engineering applications involving IC engines.

1.4 Structure of the Thesis

This thesis is structured into several chapters, starting with an introduction to the problem and its significance. Following the introduction is a comprehensive literature review discussing previous studies and methods used in the analysis of journal bearings and IC engines. The mathematical formulation of the problem and the numerical methods employed are then presented. The Algorithm and Implementation section provides a detailed explanation of the code and its functions. The results of the pressure distribution simulation and eccentricity optimization are discussed, followed by the conclusion and suggestions for future work.

Chapter 2

LITERATURE REVIEW

2.1 Literature review on Journal Bearings

Journal bearings are crucial components in rotating machinery, including four-stroke engines, where they support radial loads and facilitate smooth rotational motion. The functionality of these bearings hinges on a thin lubricant film that separates the shaft (journal) from the bearing sleeve, significantly reducing friction and wear. The efficient performance of these bearings directly impacts the overall efficiency and reliability of engines, making their study critical for mechanical engineering applications.

The study by **Chasalevris and Sfyris [3]** provides a significant advancement in the analysis of finite journal bearings by offering an exact analytical solution to the Reynolds equation, which traditionally relied on numerical methods due to its complexity. The authors are able to derive closed-form expressions for the stiffness and damping coefficients of the finite journal bearing using their analytical approach. It addresses the unique challenges posed by finite-length bearings, such as side flow effects and specific boundary conditions, and compares its analytical results with numerical solutions and earlier analytical attempts. This comprehensive approach not only validates the accuracy of the analytical methods but also enhances the understanding of the behavior and design of journal bearings.

Suryawanshi et al. [4] explores the behavior of plain circular and non-circular journal bearings, focusing on key design parameters. The paper discusses the validity of linear approximation for the oil film forces in journal bearings and analyzes the influence of critical phenomena and dynamic parameters on rotordynamic analysis, comparing experimental results with linear and nonlinear numerical models. A unique approach to thermo-hydrodynamic analysis is employed, assuming all heat generated by viscous shear is dissipated within the fluid without heat conduction through the boundaries. The research examines the impact of lubricant viscosity on various factors, including eccentricity, Sommerfeld number, load-carrying capacity, pressure distribution, frictional force, power loss, and temperature distribution. Theoretical results are validated experimentally, highlighting the importance of bearing geometry in managing thermal effects and ensuring stability. This study offers significant insights into how lubricant viscosity and bearing geometry influence the performance of hydrodynamic journal bearings. Major finding from their research is that the excitation force, particularly from rotating unbalance, is the main parameter that influences the nonlinearity of hydrodynamic bearings. For high unbalance levels, the linear model can provide inaccurate results that exceed the bearing's radial clearance.The influence of shaft internal damping, gyroscopic effect, and shaft position inside the bearing is less significant, with differences only occurring near the first natural frequency of the system.

Journal bearings are essential in machinery, providing support to rotating shafts and reducing friction through hydrodynamic lubrication. Traditionally, the performance of these bearings has been analyzed using Reynolds' equation, which assumes linear boundaries. However, real-

world applications often involve nonlinear characteristics that complicate this analysis. Recent research by **Tiago Henrique Machado et al. [5]** explores the impact of nonlinear boundaries—such as geometric, material, and operational nonlinearities - on hydrodynamic forces within journal bearings. Their work, utilizing both analytical models and numerical simulations, reveals that nonlinearities can significantly affect load-carrying capacity and stability, with potential increases or decreases in performance depending on the type of nonlinearity. This highlights the importance of incorporating nonlinear effects into performance predictions. Advances in modeling techniques, including nonlinear extensions to the Reynolds equation and advanced computational methods like finite element analysis and CFD, are improving our ability to simulate these complex behaviors. Future research will focus on integrating advanced materials and refining computational methods to enhance the accuracy of theoretical models, ensuring more reliable and efficient bearing performance.

Peng Liang et al. [6] introduced a method for measuring the hydrodynamic effect on the bearing land using the "dynamic pressure ratio (γ)", and finds that this ratio increases with eccentricity ratio and rotating speed, especially at high eccentricity ratios. Their approach emphasizes the need to accurately capture the interactions between the lubricant film and the bearing land, which significantly influence the bearing's load-carrying capacity and overall efficiency. Major findings from their research indicate that dynamic pressure ratio (γ) can be used to measure the influence of hydrodynamic effect on the bearing. Pocket pressure is the largest when the oil film thickness of this pocket is the smallest and hydrodynamic effect on bearing land of this pocket is the strongest. The researches also concluded that Dynamic pressure ratio rises as eccentricity ratio and rotating speed increase. This improved measurement capability is crucial for optimizing bearing design and performance, offering more reliable data for engineering applications and contributing to advancements in bearing technology.

2.2 Previous Studies on Pressure Distribution in Bearings

Extensive research has been conducted to understand the pressure distribution within journal bearings, a factor that dictates the load-carrying capacity and operational stability of these components. Studies employing analytical, numerical, and experimental methods have provided insights into how bearing geometry, lubricant properties, and operating conditions influence pressure distribution. Key findings highlight the importance of these parameters in optimizing bearing performance.

Najar and Harmain's [7] study provides a numerical investigation into the pressure profile within hydrodynamic lubrication thrust bearings by solving the Reynolds equation using the finite difference method (FDM). The primary objective is to analyze the pressure distribution in the lubricant oil film. The methodology involves applying FDM to the Reynolds equation, with various grid sizes considered to ensure grid independence and refine result accuracy. Key findings include the observation of pressure variations across the bearing surface, with larger pressures near the trailing edge of the pad, and the determination of film thickness based on bearing pad geometry. The study emphasizes the importance of grid refinement, showing significant changes in pressure values with finer grids, and the shifting location of peak

pressure provides insights for probe placement. The numerical results are validated against existing literature, demonstrating good agreement. This work enhances the understanding of pressure profiles in thrust bearings and underscores the vital role of numerical methods in tribology.

R. K. Sharma and R. K. Pandey [8] conducted experimental studies to investigate pressure distributions in finite slider bearings with various single continuous surface profiles (cycloidal, catenoidal, polynomial, and plane) on the pads, using both clean and contaminated lubricating oils. Their research aimed to enhance understanding of how surface profiles impact the distribution of pressure in finite thrust bearings. Major findings from their work reveal that the continuous surface profiles on the pads significantly influence pressure distribution, affecting the load-carrying capacity and stability of the bearing. The cycloidal profile pad generates the highest pressure compared to the other profiles tested (catenoidal, polynomial, and plane) under the same operating conditions. The presence of contaminants in the lubricating oil has profound effect on the pressure development in the bearing, although contaminants are undesirable. And it was found that significant reduction in pad size is possible when using a cycloidal profile pad to achieve the same load carrying capacity as other pad profiles under identical input conditions. This research provides valuable insights into the design and optimization of bearing surfaces, highlighting the importance of considering surface profile characteristics to improve bearing performance in practical applications.

Zhang et al. [9] conducted an analysis of the pressure distribution in elastohydrodynamic journal bearings under grease lubrication. The paper introduces a grease lubrication Reynolds equation based on the Herschel-Bulkley model to analyze the pressure distribution in a misaligned journal bearing, and finds that the pressure increases with rotation speed and eccentricity ratio, and the pressure distribution is symmetrical when the elastohydrodynamic (EHD) effect is not considered, and can be extremely high when both are high, requiring the use of elastohydrodynamic lubrication theory to calculate the deformation of the contact area and revise the pressure distribution model. When the EHD effect is considered, there is a second peak in the pressure distribution, and the position of this second peak moves to the right as the rotation speed or eccentricity ratio increases. Additionally, it was concluded that the maximum value of the pressure distribution might not occur at the contact point when the EHD effect is considered. This research provides valuable insights into the design and optimization of journal bearings, particularly in applications where grease lubrication is preferred due to its superior sealing properties and lower maintenance requirements.

In their study, **Yoshimoto et al. [10]** performed numerical calculations to analyze the pressure distribution within the bearing clearance of circular aerostatic thrust bearings equipped with a single air supply inlet. Their research aimed to enhance the understanding of how air pressure is distributed across the bearing surface, which is critical for the performance and stability of aerostatic bearings. The study utilized computational methods to simulate the pressure distribution, taking into account factors such as the geometry of the bearing, the position of the air supply inlet, and the flow characteristics of the air. Major findings from their research indicate that the pressure distribution is highly sensitive to the location and design of the air supply inlet, with certain configurations leading to more uniform and stable pressure profiles.

These findings are important for optimizing the design of aerostatic thrust bearings, as they suggest that careful consideration of the air inlet position can significantly improve bearing performance, reducing the risk of instability and enhancing load-carrying capacity. This study contributes valuable insights into the design and operation of aerostatic bearings, which are widely used in high-precision applications due to their low friction and wear characteristics.

2.3 Finite Difference Method (FDM) in Engineering Applications

The Finite Difference Method (FDM) is a numerical technique widely applied in fluid dynamics, heat transfer, and lubrication theory to solve differential equations by approximating them with difference equations. Its application in engineering has proven effective for modeling and simulating complex physical phenomena.

Mintu Karmakar et al. [11] focused on comparing the errors involved in calculating the journal force of a short cylindrical oil film bearing. Their research aimed to evaluate the accuracy of different computational methods used to determine the forces generated within the oil film that separates the journal from the bearing surface. The study involved a detailed analysis of various approaches, including Finite Difference Method (FDM) approach, Finite Difference Method (FDM) using matrix formation and Finite Element Method (FEM) using MATLAB PDE solver are implemented for calculation of journal forces. The paper also performs a statistical analysis using ANOVA to understand the dependency of the method, step/element size, and eccentricity on the computational time and errors. Major findings from their research highlight that the choice of numerical method (FDM, FDM matrix, or FEM using MATLAB PDE solver) and the element/grid size have a significant impact on the accuracy and computational time of calculating the journal force for a short cylindrical oil film bearing. The FDM Matrix method is more consistent and stable in terms of the absolute error compared to the conventional FDM method, but it has higher computational time. The FEM method using the MATLAB PDE solver is the most accurate and consistent in estimating the journal force, but it requires more computational time, which increases as the element size decreases. The authors emphasize the importance of selecting the appropriate computational technique based on the specific requirements of the bearing design and operational parameters. Their work provides valuable insights for engineers and researchers in selecting and refining calculation methods to improve the accuracy of force predictions in short cylindrical oil film bearings, which is crucial for optimizing bearing performance and ensuring mechanical reliability.

Fanming Meng and Yuanpei Chen [12] conducted an analysis of elasto-hydrodynamic lubrication (EHL) model of journal bearings using various numerical methods. The research aimed to compare the effectiveness and accuracy of different numerical approaches in modeling the complex interactions between elastic deformation of the bearing surfaces and the hydrodynamic pressure generated within the lubricant film. The researcher used the finite difference method to solve the Reynolds equation for the oil film pressure and Employing four different numerical methods to calculate the deformation of the bearing liner: Direct finite element method (DFEM), Influence coefficient method (ICM), Fast-Fourier transform method (FFTM) and Direct Boussinesq method (DBM). Under various operating conditions, the tribological performances evaluated by finite element method-based approaches (DFEM and

ICM) are consistent with each other, as are those assessed using Boussinesq-based approaches (FFTM and DBM). However, compared to the finite element methods, the Boussinesq-based methods tend to overestimate the friction coefficient, film thickness, and bearing deformation, while underestimating the film pressure, load-carrying capacity, and friction force. By applying multiple computational techniques, the authors sought the discrepancies between the FEM-based and Boussinesq-based methods become more significant under certain operating conditions, such as high length-diameter ratios, eccentricity ratios, rotational speeds, and lubricant viscosities. The FFTM method is the most computationally efficient among the four methods, followed by DBM and FEM based methods, can be recommended for analyzing journal bearing behavior at low pressures. The study also revealed that considering the elastic deformation of the bearing surfaces is essential for a more precise and realistic prediction of bearing performance. This research contributes significantly to the field of bearing design by offering a comparative perspective on the numerical methods available for EHL analysis, guiding researchers in selecting the most suitable approach for specific applications.

2.4 Eccentricity in Journal Bearings

Eccentricity, defined as the offset between the center of the journal and the center of the bearing, is a critical parameter in bearing performance. It influences the pressure distribution within the lubricant film, affecting the friction, wear, and load-carrying capacity of the bearing. Studies have shown that optimal eccentricity can enhance bearing performance by reducing friction and wear while maintaining stability. Controlling and optimizing eccentricity is therefore a key aspect of bearing design and operation.

Vivi Failawati et al. [13] conducted a Computational Fluid Dynamics (CFD) analysis using ANSYS Fluent software to investigate the effect of the eccentricity ratio on the pressure distribution and deformation of a journal bearing under two different lubricating oils: semi-synthetic R3 10W-30 and synthetic oil. By utilizing CFD simulations, the authors compared the performance of semi-synthetic oil R3 10W-30 and synthetic oil in terms of pressure distribution and bearing deformation. The main objective of the research to determine the better lubricant type (R3 10W-30 or synthetic oil) to minimize failure or damage to journal bearings in diesel engine applications. Major findings from their study indicate the greater the eccentricity ratio, the thinner the oil film, leading to increased bearing deformation. It was also seen that the difference in the type of lubricant also greatly influenced the results obtained on pressure and deformation. Higher viscosity lubricants, such as synthetic oils, result in higher pressure and deformation compared to lower viscosity lubricants like semi-synthetic R3 10W-30, but they also lead to lower friction. - Synthetic oil is superior to semi-synthetic R3 10W-30 for heavy load applications, but it has a higher price.

Chapter 3

Mathematical Formulation

3.1 Dynamic analysis of Model

A crucial aspect of this analysis is the examination of the resultant reaction forces in the two bearings supporting the crankshaft. These reaction forces arise due to the complex interactions between the rotating components and the structural constraints imposed by the bearings. The forces are scrutinized for their magnitude, direction, and variation over the engine's operational cycle. Understanding the resultant reaction forces in the bearings is essential for assessing the structural integrity of the engine and ensuring that the load distribution is within acceptable limits. Deviations from optimal force distributions can lead to increased wear, fatigue, and potential failure of the bearings, emphasizing the importance of this dynamic analysis.

The findings from this study contribute valuable insights into the dynamic behavior of a simple engine model, with a specific focus on the forces experienced by the bearings supporting the crankshaft. Such knowledge is instrumental in refining the design and operational parameters of internal combustion engines, ultimately enhancing their reliability and performance.

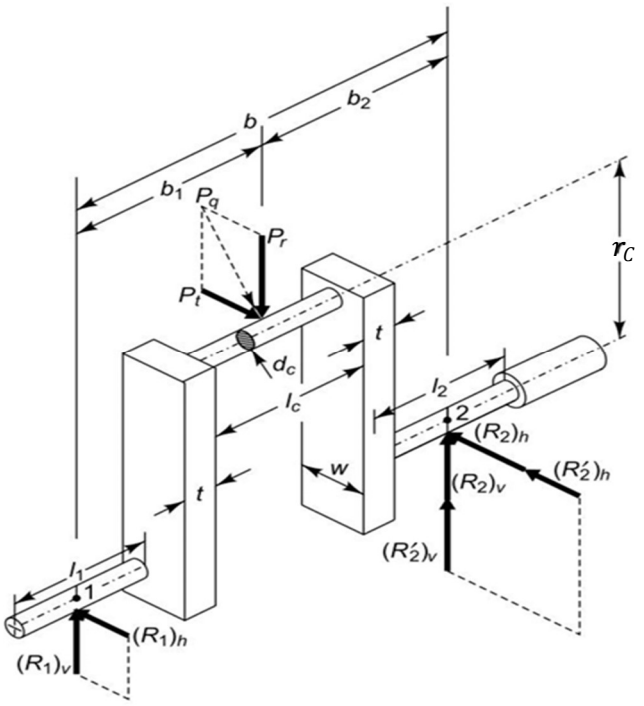

Figure 1. Crank Pin and Web
(**Source:** Bhandari, V.B.,"Design of Machine Elements, 3e")

Assumptions:

(i) The engine is vertical and the Centre crank shaft is at the maximum torque condition. (The torque is maximum when the tangential component of force on the crank pin is maximum. For this condition, the crank angle from the top dead centre position (q) is usually 25° to 35° for petrol engines and 30° to 40° for diesel engines.)
(ii) The crankshaft is simply supported on bearings.
(iii) Neglecting the Inertia forces associated with the systems.
(iv) Neglecting the Friction Force involved with the End Bearings.
(v) The Gas pressure is assumed to be linear throughout the power stroke.
(vi) Neglecting dynamic loading effects, temperature variations, and material nonlinearity.

(vii) It is assumed that by exclusively employing moment balance, the determination of bearing reactions can be achieved without the necessity of energy balance considerations, simplifying the analytical process.
Additionally, the combustion undergoes a process of storage within the flywheel, poised to be utilized in subsequent cycles of the engine operation, so this energy storage mechanism elucidates the recurring pattern observed in the engine's operation, wherein a repeated curve manifests after every 180 degrees of crank rotation. This recurrence underscores the cyclical nature of energy utilization and distribution within the engine

Suppose p' is the gas pressure on the piston top for maximum torque condition.

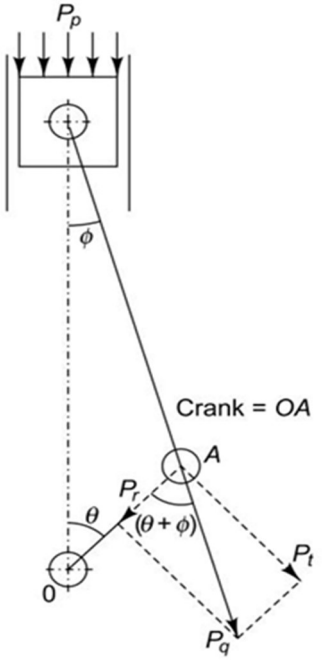

Figure 2. Force acting on crank
(**Source:** Bhandari, V.B.,"Design of Machine Elements, 3e")

$$P_p = p'.(\pi/4)d^2 \quad \textbf{... (1)}$$

The relationship between ϕ and θ is given by,

$$\sin\phi = \frac{\sin\theta}{(L_C/r_C)} \quad \textbf{... (2)}$$

$$\text{Or,} \quad \tan(\theta + \phi) = \frac{P_t}{P_r} \quad \textbf{... (3)}$$

.

So, we can write

$$\cos\phi = \left[1 - \left(\frac{r_C .sin\theta}{L_C}\right)^2\right]^{0.5} \quad \textbf{... (4)}$$

Where (L_C/r_C) is the ratio of length of the connecting rod to the radius of the crank.

The thrust on the connecting rod ($\boldsymbol{P_q}$) is given by,

$$P_q = \frac{P_p}{cos\phi} \quad \textbf{... (5)}$$

$\boldsymbol{P_t}$ and $\boldsymbol{P_r}$ are tangential and radial components of $\boldsymbol{P_q}$ at the crank pin. Therefore,

$$P_t = P_q \sin(\theta + \phi)$$

$$\text{Or,} \quad P_t = P_p \sin\theta \left(1 + \frac{\cos\theta}{\sqrt{(L_C/r_C)^2 - (\sin\ )^2}}\right) \quad \textbf{... (6)}$$

$$\text{And,} \quad P_r = P_q \cos(\theta + \phi)$$

$$\text{Or,} \quad P_r = P_p \left(\cos\theta - \frac{\sin\theta}{\sqrt{(L_C/r_C)^2 - (\sin\theta)^2}}\right) \quad \textbf{... (7)}$$

Bearing Reactions The forces acting on the centre crankshaft at an angle of maximum torque are shown in Figure 3. The crankshaft is supported on two bearings 1, 2. It is assumed that the portion of the crankshaft between bearings 1 and 2 is simply supported on bearings and subjected to tangential force $\boldsymbol{P_t}$ and radial force $\boldsymbol{P_r}$ at the crank pin as shown in Fig. 1.2. Due to the tangential component $\boldsymbol{P_t}$, there are reactions $(R_1)_H$ and $(R_2)_H$ at bearings 1 and 2 respectively. Similarly, due to the radial component $\boldsymbol{P_r}$, there are reactions $(R_1)_v$ and $(R_2)_v$ at bearings 1 and 2 respectively.

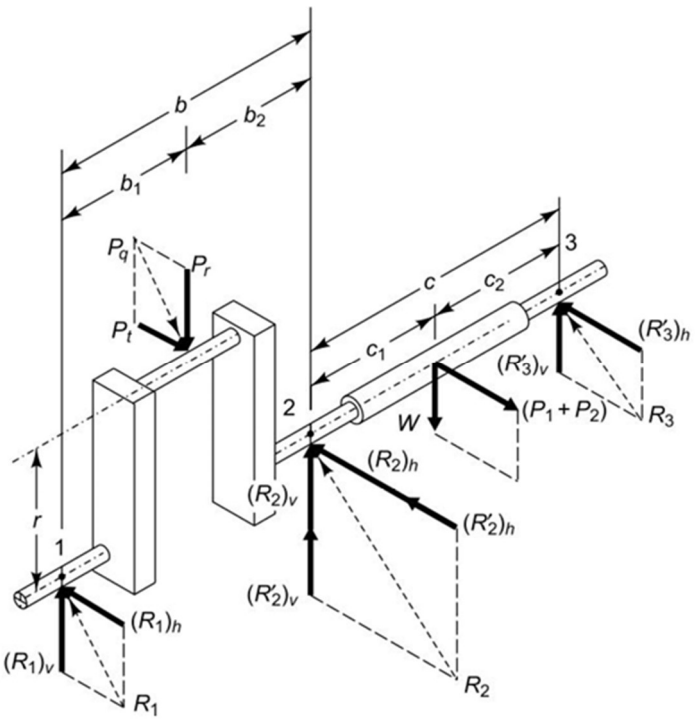

Figure 3. *Centre Crankshaft at Angle of Maximum Torque*
(**Source:** Bhandari, V.B.,"Design of Machine Elements, 3e")

Now, taking moment of horizontal forces about bearing 1,

$$P_t b_1 = (R_2)_h\, b$$

Or, $(R_2)_h = (P_t b_1)/b$

Taking moment of horizontal forces about the bearing 2,

$$P_r b_2 = (R_1)_h\, b$$

Or, $(R_1)_h = (P_t b_2)/b$

Similarly, it can be proved that

$$(R_2)_v = (P_t b_1)/b$$

$$(R_1)_v = (P_r b_2)/b$$

So, the horizontal reaction force on the bearing 1 & 2 will be the same due to symmetry.

.

Assuming bearing 1 & bearing 2 are at equidistance w.r.t Crank, along crank shaft.

Thus, $b_1 = b_2 = \frac{b}{2}$

$$\boxed{(R_1)_h = (R_2)_h = P_t/2} \quad \textbf{... (8)}$$

$$\text{Or,} \quad (R_1)_h = (R_2)_h = \frac{P_q}{2} \sin(\theta + \phi)$$

Now we can write the resultant reactions on main journal in terms of Force exerted on the Piston *(P_p)*

$$(R_1)_h = (R_2)_h = \frac{P_p}{2} \sin\theta \left(1 + \frac{\cos\theta}{\sqrt{(L_C/r_C)^2 - (\sin\theta)^2}}\right) \quad \textbf{... (9)}$$

Similarly,

$$(R_1)_v = (R_2)_v = P_r/2 \quad \textbf{... (10)}$$

Or, $(R_1)_v = (R_2)_v = \frac{P_q}{2} \cos(\theta + \phi)$

$$(R_1)_v = (R_2)_v = \frac{P_p}{2} \left(\cos\theta - \frac{\sin\theta}{\sqrt{(L_C/r_C)^2 - (\sin\theta)^2}}\right) \quad \textbf{... (11)}$$

where, $L_C/r_C = 4.5$, $cos\phi = \left[1 - \left(\frac{r_C \sin\theta}{L_C}\right)^2\right]^{0.5}$

[[1] Example 25.18 chapter-Design of IC Engine Components (Source: Bhandari, V.B.,"Design of Machine Elements, 3e")

Cylinder bore = 125 mm

(L_C/r_C) ratio = 4.5

Maximum gas pressure (p_{max}) = 2.5 MPa

Length of stroke = 150 mm

Weight of flywheel cum belt pulley = 1 kN

The torque on the crankshaft is maximum when the crank turns through 25° from the top dead centre and at this position the gas pressure inside the cylinder is 2 MPa (p'). The belts are in the horizontal direction.]

Now in our analytical model we assume the Gas pressure on Piston shows the linear characteristics. (For Power/combustion stroke**)**

Hence, we can write, $P_p = -mx + C$

Case I: When the crank is at Top dead centre position and subjected to maximum bending and no torsional moment,

i.e., at $x = 0$ or $\theta = 0$, Maximum pressure condition will be achieved inside engine cylinder. So, Maximum Thrust force,

$$P_p = p_{max} \cdot (\pi/4) d^2$$

Therefore, C = $p_{max} \cdot (\pi/4) d^2$

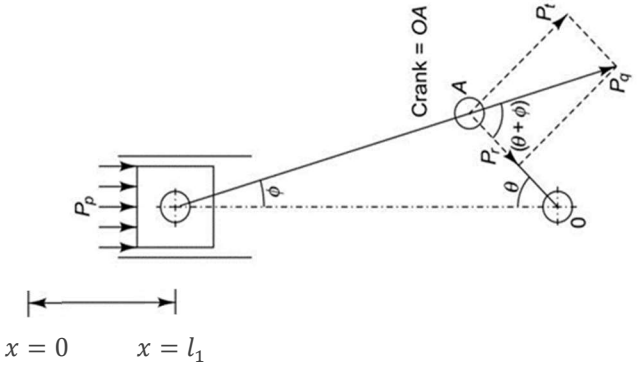

Figure 4. Force acting on crank
(**Source:** Bhandari, V.B.,"Design of Machine Elements, 3e")

Case II: When the crank is at an angle (θ_1) with line of the dead centre position and subjected to maximum torsional condition

Thrust force on piston head, $P_p = p' \cdot (\pi/4) d^2$ at, $x = r_C\,(1 - cos\theta_1) = l_1$

(p' is the gas pressure on the piston top for maximum torque condition.)

Again, $p' \cdot (\pi/4) d^2 = -ml_1 + p_{max} \cdot (\pi/4) d^2$

or, $m = \dfrac{p_{max} \cdot (\pi/4) d^2 - p' \cdot (\pi/4) d^2}{l_1}$

Now we can write,

$$P_p = \frac{p' \cdot (\pi/4) d^2 - p_{max} \cdot (\pi/4) d^2}{r_C(1-\cos\theta)} x + p_{max} \cdot (\pi/4) d^2 \qquad \textbf{... (12)}$$

Putting the value of p_{max}, p', r_C = l/2 =75 mm (where l is stroke length) and piston dia.(d) = 125 mm we get,

$$P_p = \left(\frac{(2-2.5)\pi \times 125^2}{(1-\cos 25) \times 75}\right) \times 75(1 - \cos\theta) + 2.5\,(\pi/4) 125^2$$

Or, $\boxed{P_p = 30679.615 + 65490.21479(cos\theta - 1)\ \text{N}}$ **... (13)**

For, $0 \leq \theta \leq \pi/2$

Now we get this formula of P_p which is now only the function of crank angle.

From this equation we can observe the variation of Force exerted on the piston throughout a complete cycle by putting the value of P_p which is now only the function of crank angle. Now putting the expression of P_p in equation no. 9 & 11, we can observe the variation of Resultant Reaction Force on both the bearings throughout Power stroke.

But there are some added forces associated with the bearing 2 for the attachment of Flywheel and belt arrangement.

From the reference we can write the equations for bearing 2 and 3 – by symmetry we can write

$$(R_2')_v = (R_3')_v = \frac{W}{2} = \frac{1000}{2} = 500\ N$$

$$(R_2')_h = (R_3')_h = \frac{P_1 + P_2}{2} = \frac{2000}{2} = 1000\ N$$

Now the Resultant Reaction Force on bearing 1 can be calculated by:

$$R_1 = \sqrt{\left[(\boldsymbol{R_1})_h\right]^2 + \left[(\boldsymbol{R_1})_v\right]^2} \qquad \textbf{... (14)}$$

Now the Resultant Reaction Force on bearing 2 can be calculated by:

$$R_2 = \sqrt{\left[(R_2)_v + \left(R_2'\right)_v\right]^2 + \left[(R_2)_h + \left(R_2'\right)_h\right]^2} \qquad \textbf{... (15)}$$

By putting the value of $(R_2)_v$ & $(R_2)_h$we can write the Resultant Reaction Force on bearing 2 in terms of P_p**.**

Resultant Reaction Force in bearing 3 we can write,

.

$$R_3 = \sqrt{\left[\left(R_3'\right)_v\right]^2 + \left[\left(R_3'\right)_h\right]^2} \qquad \textbf{... (16)}$$

Here the value of R_3 is constant throughout the cycle.

Plotting of Variation of P_p, $(R_1)_h$, $(R_1)_v$ & Resultant Reaction on bearings (R_1 & R_2) with different Crank Position for the entire Cycle:

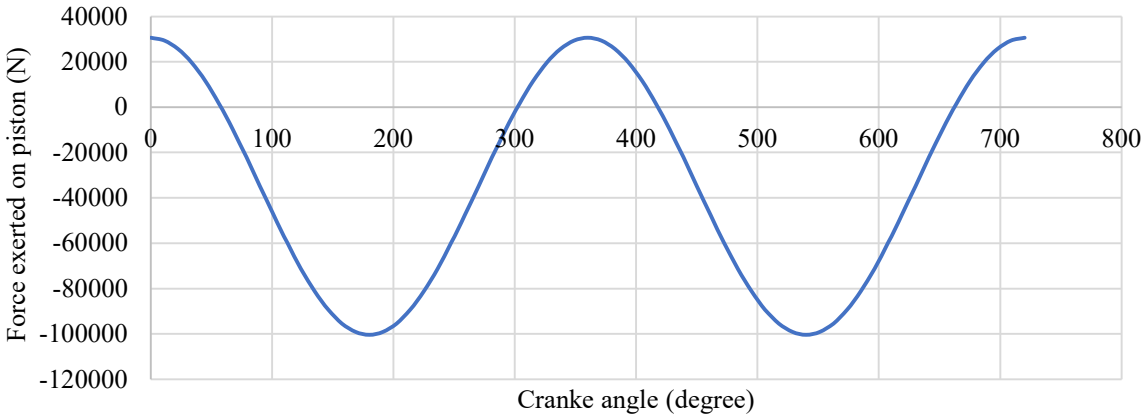

Figure 5. Force exerted on piston (P_p) VS Crank angle

The graph shown in figure 5 presents a sinusoidal representation of the force exerted on the piston as a function of the crank angle. Although the actual force profile in a four-stroke engine varies significantly during each of the cycles—intake, compression, power, and exhaust—the plot assumes a simplified model where the gas pressure on the piston exhibits linear characteristics, particularly during the power stroke. This assumption allows for a more tractable analysis of the engine's dynamics, resulting in the sinusoidal pattern observed. While this idealized representation facilitates the study of pressure distribution and bearing reactions, it is important to note that it abstracts some of the complexities inherent in the engine's atual operation.

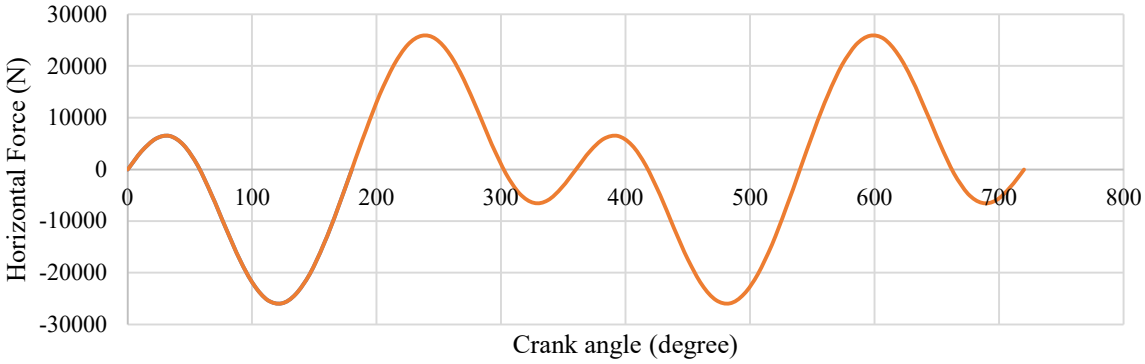

Figure 6. Horizontal reaction force $(R_1)_h$ VS Crank angle

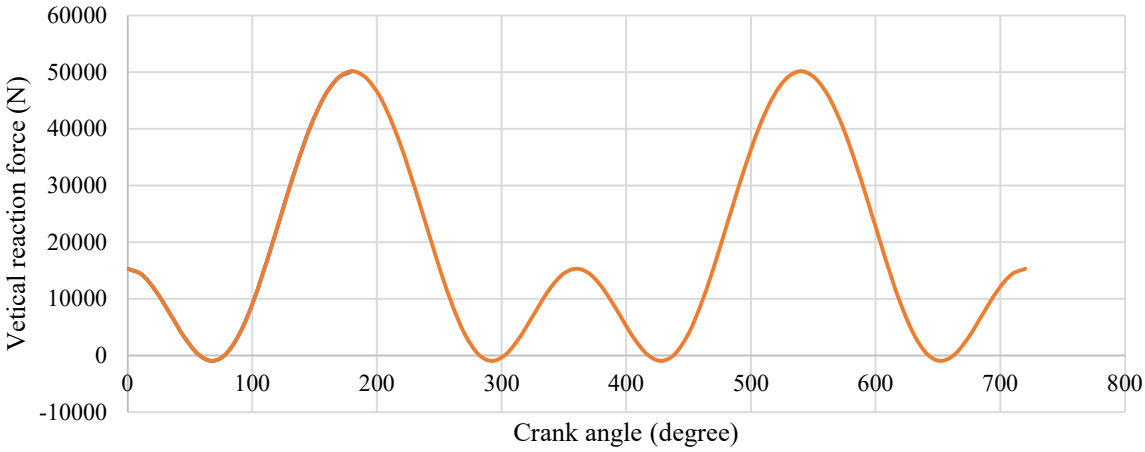

Figure 7. Vertical reaction force $(\boldsymbol{R_1})_v$ VS Crank angle

These graphs in Figure 6 & Figure 7 represent the horizontal and vertical reaction forces as functions of the crank angle in an engine assuming a simplified model where the gas pressure on the piston exhibits linear characteristics, particularly during the power stroke.

Both forces exhibit a cyclic pattern, consistent with the nature of rotating Crank shaft where forces change periodically with each cycle. The vertical reaction force has a larger amplitude compared to the horizontal force, indicating stronger forces in the vertical direction. The frequency of oscillation appears consistent across both graphs, aligning with the crankshaft's rotational frequency.

These graphs are typically used in analyzing the dynamics of internal combustion engines, where the forces generated by the pistons during the power strokes are transmitted through the crankshaft, leading to varying forces in different directions.

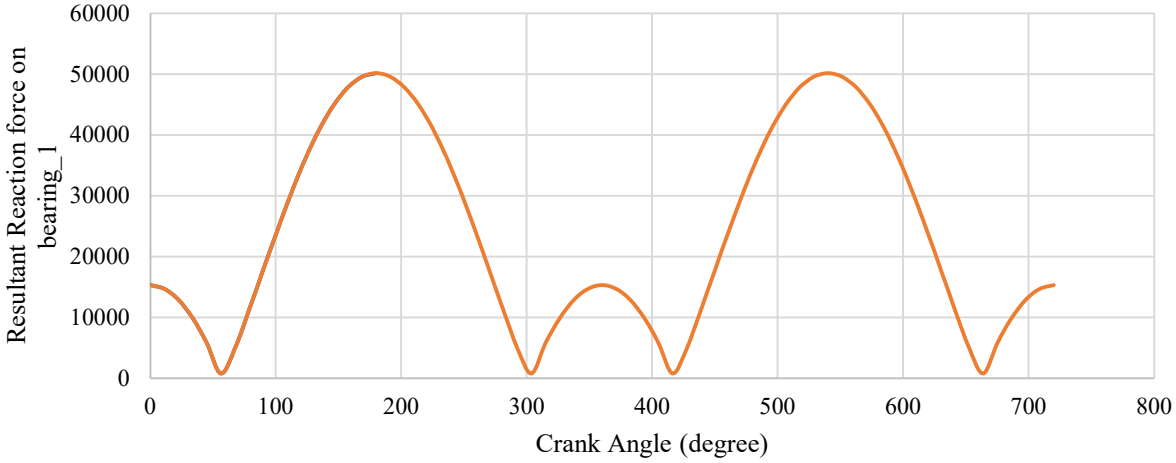

Figure 8. Resultant reaction on bearing 1 ($\boldsymbol{R_1}$) VS Crank angle

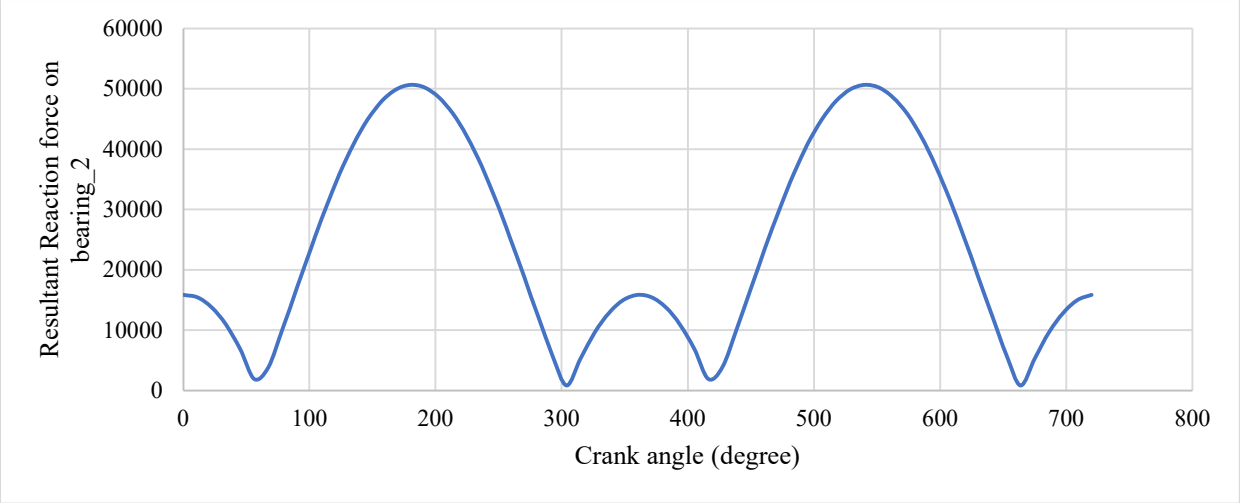

Figure 9. Resultant reaction on bearing 2 ($\boldsymbol{R_2}$)VS Crank angle

These graphs in Figure 8 & Figure 9 represent the periodic resultant reaction force on bearing 1 & bearing 2 as functions of the crank angle. The peaks and troughs observed in the graph can be attributed to the power stroke and other phases of the engine cycle. The simplified assumption of linear gas pressure during the power stroke provides a reasonable explanation for the general shape of the curve.

3.2 Simulation for pressure distribution using Numerical Method

The numerical methods used in the program primarily focus on solving the Reynolds equation for pressure distribution in journal bearings. These methods are essential for predicting the behavior of the lubricant film within the bearing under various operating conditions. Below is a detailed elaboration of the numerical methods employed:

3.2.1 Reynolds Equation for Journal Bearings

The Reynolds equation, a fundamental equation in lubrication theory, describes the pressure distribution in the lubricant film of journal bearings.

3.2.1.1 Model of Journal Bearing

Hydrodynamic bearings are crucial components in internal combustion (IC) engines, serving as main bearings that support and allow the rotation of the crankshaft. These bearings rely on the generation of a hydrodynamic film of lubricant between the rotating and stationary surfaces to provide load support and reduce friction.

The journal bearing geometry utilized in this study is depicted in Figure 10. The bearing center is denoted as O', while O represents the journal or shaft center. The eccentricity between the shaft and bearing centers is indicated by 'e', and 'L' is the length of the bearing. An external load 'W' is considered to act vertically along the Y-axis and remains constant. The hydrodynamic pressure generated in the convergent region creates a fluid film that separates the bearing from the shaft and counterbalances the external force acting on the shaft. In this region, the fluid properties remain unchanged.

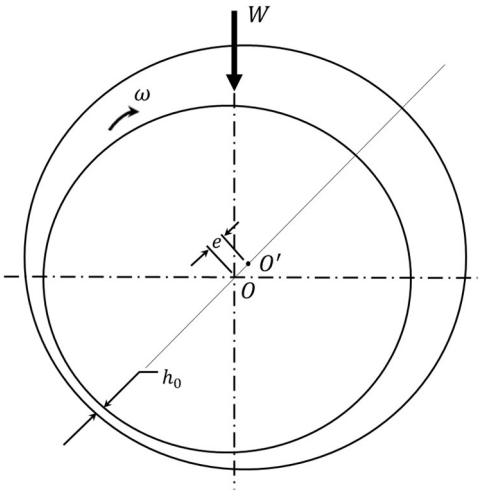

Figure 10. journal bearing geometry

3.2.1.2 Reynolds Equation for finite length bearing

For finite length journal bearings, analytical solutions are not possible and numerical methods are used. Here a numerical solution of two- dimensional Reynolds equation for a finite journal bearing is presented.

The generalized differential Reynolds equation for Iso-viscous, incompressible & laminar flow of Newtonian fluid considered as –

$$\frac{\partial}{\partial s}\left(\frac{h^3}{\mu}\frac{\partial p}{\partial s}\right)+\frac{\partial}{\partial z}\left(\frac{h^3}{\mu}\frac{\partial p}{\partial z}\right)=6U\frac{\partial h}{\partial s}+12\frac{\partial h}{\partial t} \quad \text{... (17)}$$

Then non-dimensional differential expression of Reynolds equation can be written as –

$$\frac{\partial}{\partial \bar{S}}\left(H^3\ \frac{\partial \bar{P}}{\partial \bar{S}}\right)+\frac{\partial}{\partial \bar{z}}\left(H^3\ \frac{\partial \bar{P}}{\partial \bar{Z}}\right)=\frac{6U\mu R}{p_0 c^2}\left(\frac{\partial \bar{H}}{\partial \bar{S}}+\frac{2}{\omega}\ \frac{\partial H}{\partial t}\right) \quad \textbf{... (18)}$$

Where,

$$\bar{P}=\frac{p-p_0}{p_{ref}}\ ,\quad p_{ref}=\frac{6U\mu R}{p_0 c^2}\times p_0=\frac{6\omega\mu R^2}{c^2}\ ,\quad \bar{z}=\frac{z}{R}\ ,\ \bar{s}=\frac{s}{R}\ ,\ H=\bar{h}=\frac{h}{c}$$

$$\omega=\frac{U}{R}\ ,\ s=R\theta,$$

$$H=\bar{h}=\frac{h}{c}=1-\varepsilon\cos(\theta-\emptyset)$$

$$\frac{\partial H}{\partial \bar{S}}=\varepsilon\sin(\theta-\emptyset)$$

$$\frac{\partial H}{\partial t}=-\dot{\varepsilon}\cos(\theta-\emptyset)-\ \varepsilon\dot{\emptyset}\sin(\theta-\emptyset)$$

3.3 Derivation of Discretized Form Using FDM

The Reynolds equation is discretized using the Finite Difference Method. Partial derivatives are approximated with finite differences, and a finite difference grid is formed to solve the equation numerically.

Using the Finite Difference Method (FDM), equation (18) can be reformulated in a manner similar to the approach described by **Huang [14]**.

$$A\ \bar{P}_{i-1,j}+B\ \bar{P}_{i,j-1}+\ C\ \bar{P}_{i,j}+\ D\ \bar{P}_{i+1,j}+\ E\ \bar{P}_{i-1,j}=F \quad \textbf{... (19)}$$

Where,

$$A=\ H^3_{1+\frac{1}{2}}\ ,\ B=\ H^3\ ,\ D=\ H^3_{1-\frac{1}{2}}$$

$$C=\ -(A+D+2B)$$

$$E=\ B$$

$$F=\Delta s^2\left[\varepsilon\sin(\theta-\emptyset)-\left(\frac{2}{\omega}\right)\left(\dot{\varepsilon}\cos(\theta-\emptyset)+\ \varepsilon\dot{\emptyset}\sin(\theta-\emptyset)\right)\right]$$

$$H=\ 1-\varepsilon\cos(\theta-\emptyset)$$

$$H_{ip}=\ H_{1+\frac{1}{2}}=1-\varepsilon\cos(\theta+0.5\times\Delta s-\emptyset)$$

$$H_{im}=\ H_{1-\frac{1}{2}}=1-\varepsilon\cos(\theta-0.5\times\Delta s-\emptyset)$$

3.4 Pressure Distribution Simulation by iteration using FDM

The pressure distribution is simulated by iteratively solving the discretized Reynolds equation using FDM. The initial guess for the pressure distribution is updated in each iteration until convergence is achieved, based on the specified boundary conditions and convergence criteria.

$$\bar{P}_{i,j} = \frac{F - A\,\bar{P}_{i-1,j} - B\,\bar{P}_{i,j-1} - D\,\bar{P}_{i+1,j} - E\,\bar{P}_{i-1,j}}{C} \quad \text{... (20)}$$

In this project, the finite difference method (FDM) is applied to solve the pressure distribution in a journal bearing, particularly focusing on the iterative process. The pressure equation (19) is rewritten in the form of equation (20), where the pressure at a grid point is calculated using the pressures at surrounding points, weighted by coefficients derived from the bearing's geometry and operational conditions. The iterative solution begins with an initial pressure of 0.5 at all nodes within the fluid film. A relaxation technique is employed, where 30% of the current pressure estimate is combined with 70% of the previous estimate to improve convergence stability. The iterative process continues until the fractional relative error between successive iterations falls below 10^{-4} with a maximum iteration limit set at 3000. This method ensures accurate pressure distribution calculations, critical for understanding bearing performance.

3.5 Convergence Criteria and Error Analysis

Convergence is achieved when the changes in pressure values between successive iterations fall below a specified threshold. Error analysis is performed to ensure the accuracy and stability of the solution. The relative and absolute errors are monitored to guide the iterative process.

The convergence criteria and error analysis in the code are crucial for ensuring that the numerical solution obtained from the simulation is accurate and stable. The convergence criteria and error analysis in two main parts:

3.5.1. Convergence Criteria in Pressure Distribution Calculation in the 'conventional_FDM_iteration_with_boundary_conditions' function

3.5.2. Optimization Convergence in the Eccentricity Calculation in the 'my_function' and 'fmin' function

3.5.1. Convergence Criteria in Pressure Distribution Calculation

This part of the code is responsible for iterating through the pressure values in the finite difference method (FDM) until the solution stabilizes, meaning the changes between successive iterations are negligible.

Convergence Criteria:

- Relative Error Calculation:

The code calculates the relative error between the current pressure matrix 'P' and the previous iteration's matrix 'P_previous'. This error tells us how much the pressure values are changing from one iteration to the next.

```
relative_error = np.where(np.logical_or(np.abs(P) < 0.00000001, np.abs(P_previous) < 0.00000001),
      0,
      ((P - P_previous) / np.maximum(np.abs(np.maximum(P_previous, P)), 0.0001))
  ).astype(np.float64)
```

The np.where function is used to avoid division by very small numbers, which can cause numerical instability. Specifically, if P or P_previous is very close to zero (less than 1e-8), the relative error for that point is set to 0.

Generally, the relative error at each point can be calculated using the formula:

$$relative\_error = \frac{P - P_{previous}}{\max\left(abs\left(\max\left(P, P_{previous}\right)\right), 0.0001\right)}$$

This formula ensures that the relative error is normalized and avoids division by zero by setting a small minimum value (0.0001).

- RMSE (Root Mean Square Error):

The relative errors are then aggregated into a single metric using RMSE, which gives a measure of the average error magnitude across the entire pressure matrix.

```
    rmse_relative_error = np.sqrt(np.mean(relative_error 2))
```

- Scaling for Large Errors:

If any relative error exceeds 1, the code scales down the relative error values. This scaling prevents instability and keeps the errors within a manageable range.

```
  if max_value > 1:
      relative_error /= max_value
      rmse_relative_error = np.sqrt(np.mean(relative_error 2)) max_value
```

- Convergence Check:

The iteration loop checks if the RMSE of the relative error falls below a predefined threshold ('min_relative_error'). If the error is sufficiently small, it indicates that the solution has stabilized, and the loop breaks.

```
  if rmse_relative_error < min_relative_error:
      break
```

3.5.2. Optimization Convergence in the Eccentricity Calculation

In the latter part of the code, the goal is to find the eccentricity ratio (‘epsilon’) that minimizes the difference between the calculated bearing force and a target bearing force (‘Bearing_force0’).

Optimization Convergence Criteria:

- Objective Function (‘my_function’):

This function returns the absolute difference between the calculated bearing force and the target bearing force. The optimization process aims to minimize this difference.

```
return np.abs(Bearing_force0 - Bearing_force)
```

- Optimization using ‘fmin’:

The ‘fmin’ function from SciPy is used to find the eccentricity value that minimizes the objective function. This function uses the Nelder-Mead simplex algorithm, which iteratively refines the solution based on the function’s values at various points.

```
x_min = fmin( my_function, x0, args=(...),  xtol=0.02, ftol=1 , ...)
```

- Tolerance (‘xtol’ and ‘ftol’):

The ‘xtol’ and ‘ftol’ parameters set the convergence thresholds. ‘xtol’ is the acceptable tolerance for changes in the parameter ‘x’ (eccentricity), and ‘ftol’ is the tolerance for changes in the function value. When these values fall below the set thresholds, the algorithm considers the solution converged.

Hence, The pressure distribution calculation iteratively refines the pressure values using a relative error criterion until the solution stabilizes (RMSE of relative error falls below a threshold) and the eccentricity calculation uses an optimization process to find the value that minimizes the difference between the calculated and target bearing forces, with convergence determined by tolerance settings (‘xtol’ and ‘ftol’).

These convergence criteria ensure that the simulation results are both accurate and computationally efficient.

3.6 Calculation of Bearing Number and Sommerfeld Number

The bearing number and Sommerfeld number are dimensionless parameters used to characterize journal bearing performance. They are calculated using the pressure distribution obtained from the numerical solution of the Reynolds equation.

The bearing number is given by:

$$Bearing\ Number = \frac{6\mu\omega R^2}{P_0 c^2}$$

The Sommerfeld number is related to the eccentricity ratio and provides insights into the lubrication regime. This dimensionless number characterizes the operating conditions of journal bearings, taking into account factors like load, viscosity, speed, and clearance. A higher Sommerfeld number generally indicates a lower load-carrying capacity or higher stability in the bearing. The Sommerfeld number is given by:

$$Sommerfeld\ Number = \frac{0.5}{\pi}\left(\frac{(R-c)^2}{c^2}\right)\frac{\mu\omega L_d 4R^2}{Bearing\ Force}$$

Where,

$$Bearing\ Force = P_0 R^2 \times Bearing\ Number \times \sqrt{{F_x}^2 + {F_y}^2}$$

Chapter 4

Flowcharts and Implementation

4.1 Flowcharts

Flowcharts are provided to illustrate the algorithm and the logical flow of the code. These visual aids help in understanding the implementation details and the interactions between different functions.

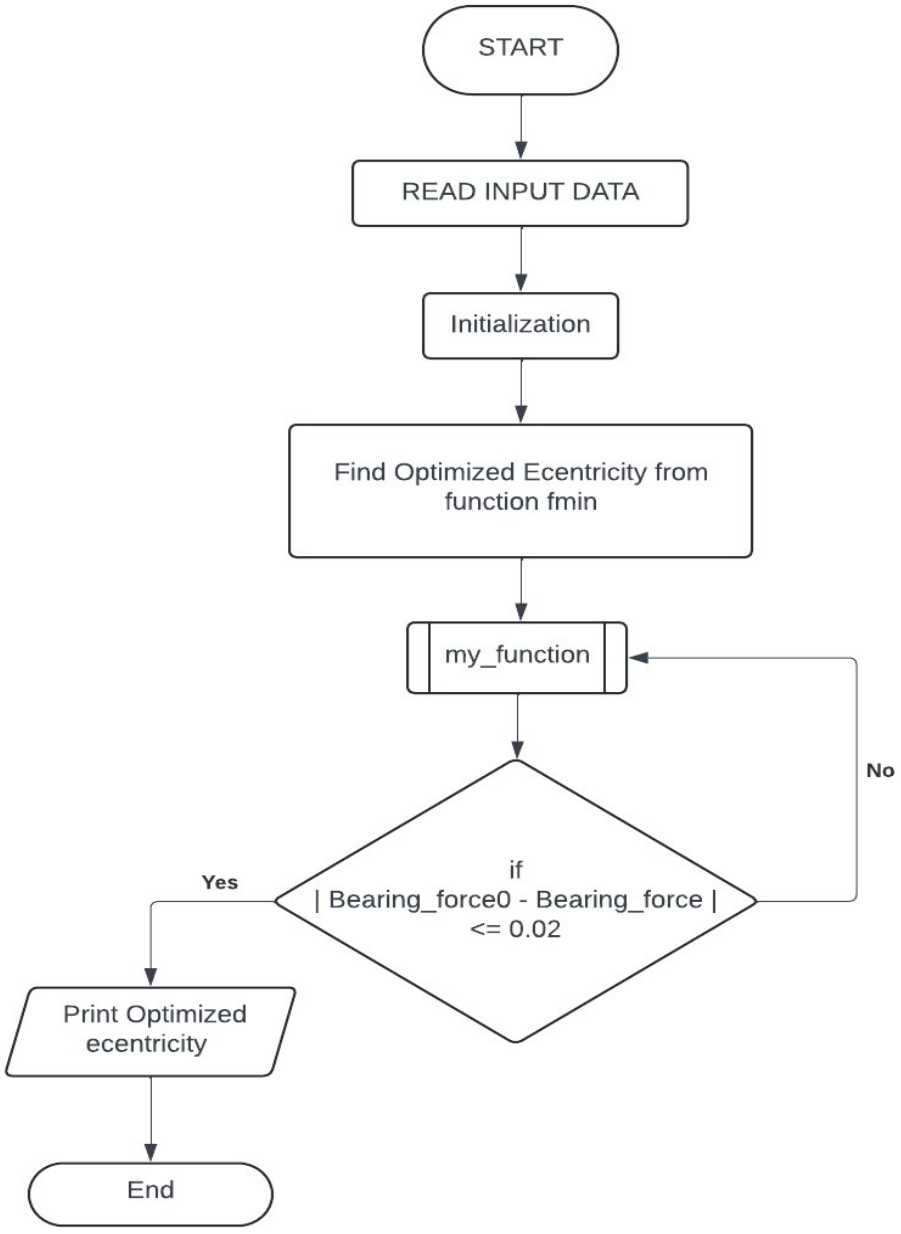

Figure 11. Flowchart of the program

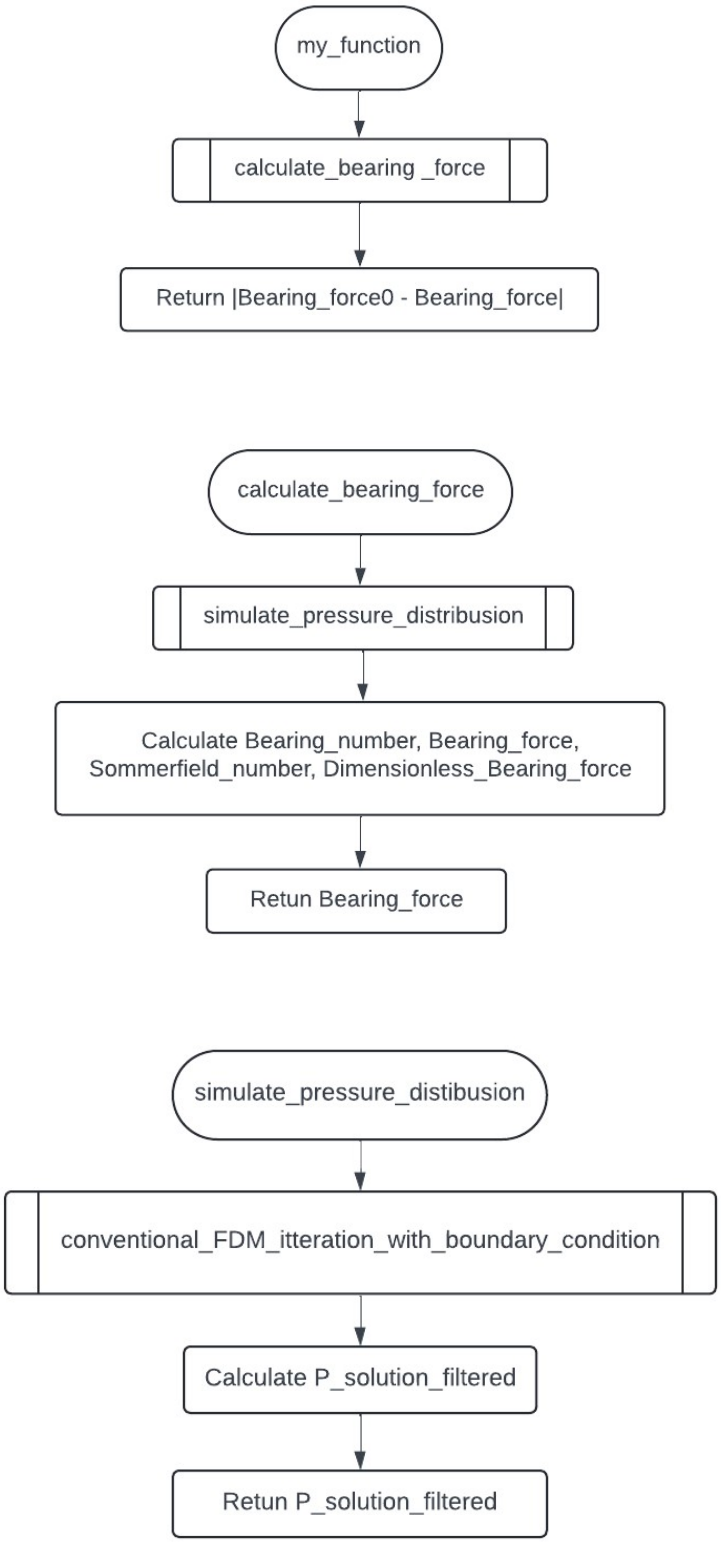

Figure 12. Flowchart of the program (Functions - 1)

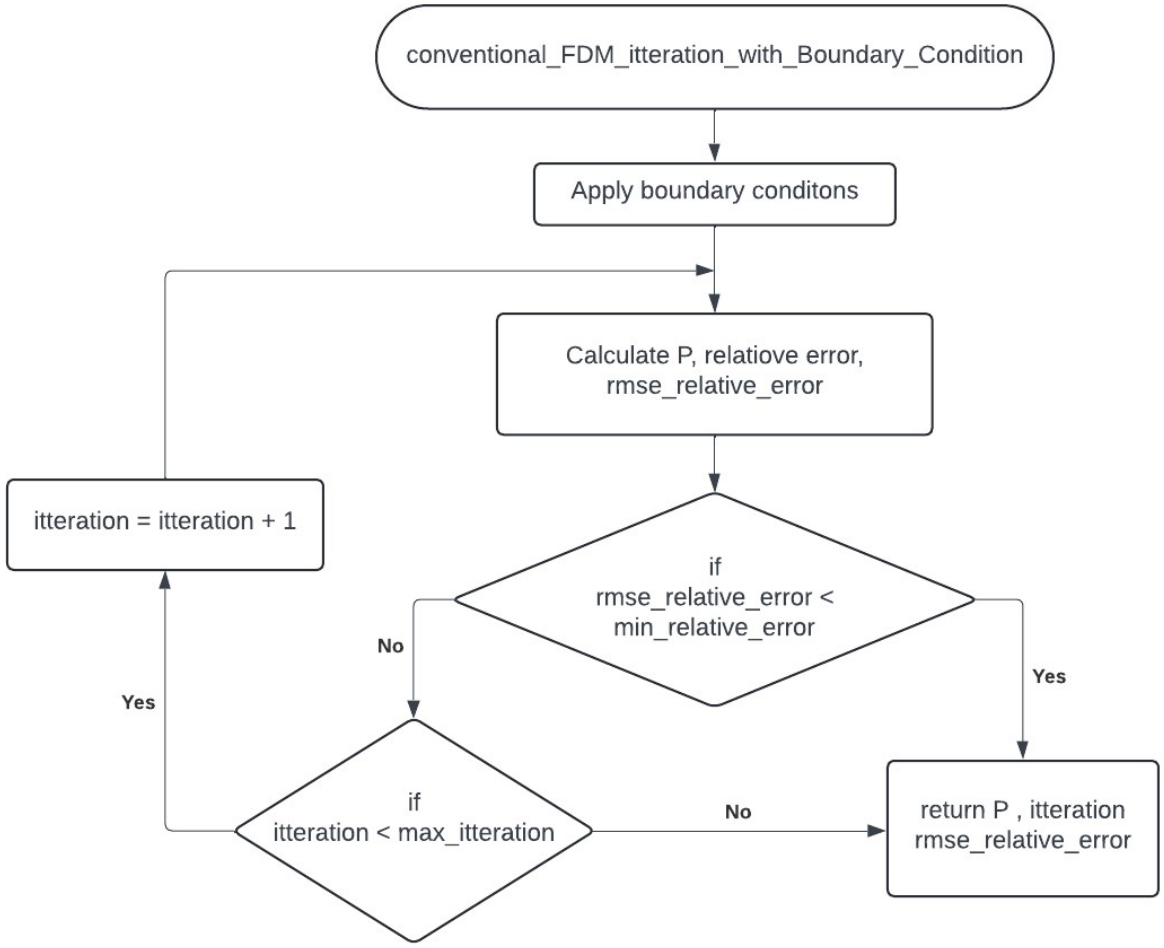

Figure 13. Flowchart of the program (Function - 2)

4.2 Overview of the Code

The computational model is implemented in Python, utilizing libraries such as NumPy for numerical computations and SciPy for optimization. The code is structured into functions, each responsible for a specific task in the simulation and optimization process.

The main purpose of the code used in this project is to calculate the bearing force, Sommerfeld number, and other parameters for a journal bearing based on given inputs such as eccentricity, phase angle, rotational speed, bearing dimensions, and lubricant properties. The code uses the finite difference method to simulate the pressure distribution on the bearing surface and then calculates the bearing force from this distribution. It uses FDM with relaxation method to improve convergence stability and includes functionality for optimization to improve the accuracy and efficiency of the calculations. Overall, this code is useful for analyzing and designing journal bearings in rotating machinery systems.

Chapter 5

Results and Discussion

Initially, we employed a Finite Difference Method (FDM) to compute the pressure distribution across the bearing surface. This involved solving the Reynolds equation while applying the Half-Sommerfeld boundary condition. Subsequently, we conducted an analysis on the performance characteristics of the full journal bearing.

5.1 Simulation Results for Pressure Distribution

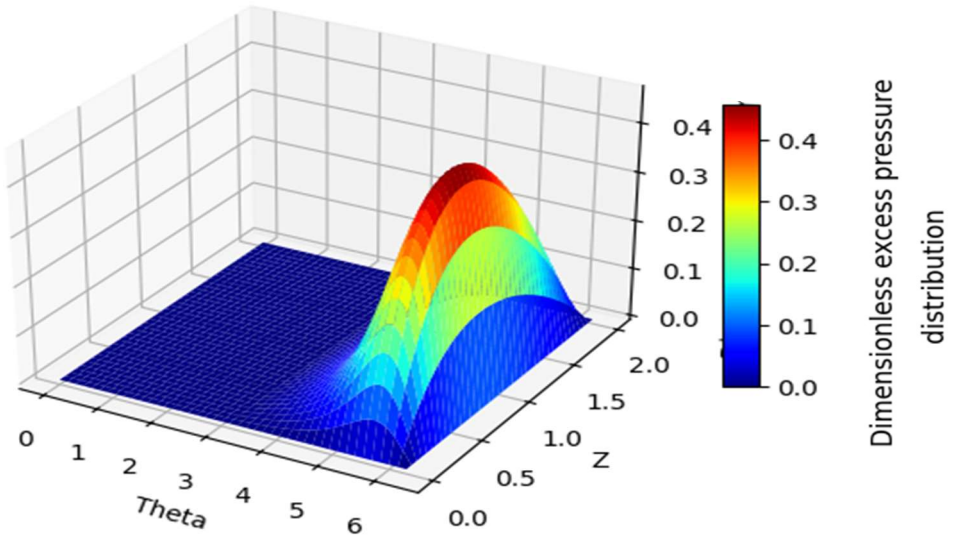

Figure 14. Dimensionless excess pressure distribution in a journal bearing

This graph represents a 3D plot of the dimensionless excess pressure distribution in a journal bearing, showing how the pressure varies across the bearing surface along axial and radial positions for a defined eccentricity ratio of 0.5, length-to-diameter (L/D) ratio of 1, and specific operating conditions.

The high-pressure region (red) is critical for bearing performance, as it supports the load carried by the journal bearing. The location and magnitude of this peak can influence the bearing's ability to support the shaft and reduce wear. The regions where the pressure is lower (blue) indicate areas of the bearing surface where the load support is minimal. These areas can be prone to cavitation or other issues if the pressure drops too much.

This visualization helps in understanding the complex pressure distribution within a journal bearing, providing insights into how the bearing will perform under different operating conditions. This pressure distribution aids in predicting the journal's position iteratively by determining the eccentricity-induced displacement of the journal centre along with the attitude angle.

This pressure distribution analysis is crucial for the design and optimization of journal bearings in engines and other rotating machinery, ensuring that the bearing can adequately support the load and operate reliably.

5.2 Effect of Various Parameters on Bearing Performance

In this study we have got following graphs, collectively highlight the dynamic behavior of journal bearings within an engine, emphasizing the importance of considering both L/D ratios and crank angle-dependent variations when designing and analyzing bearing performance.

5.2.1 Results and plotting of sommerfeld number Vs Eccentricity ratio for different L/D ratio:

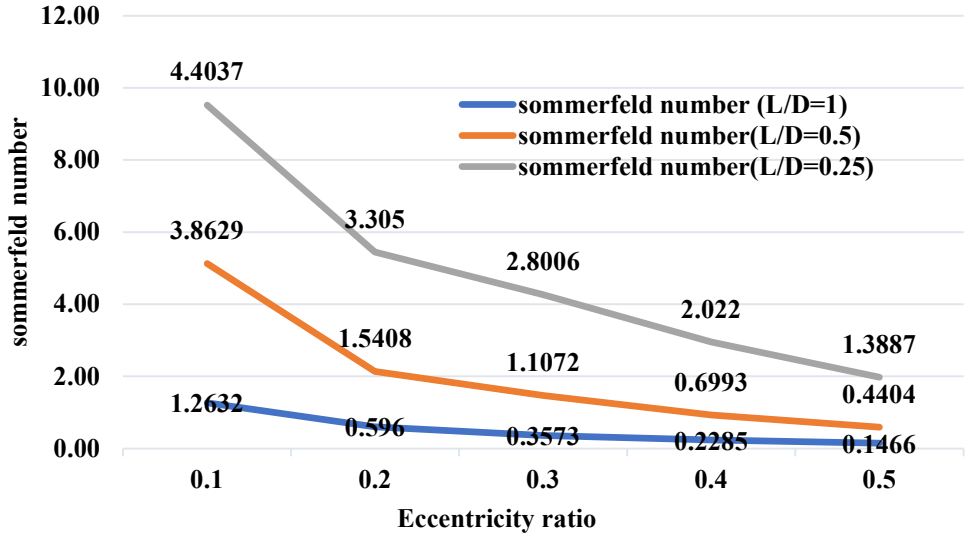

Figure 15. Sommerfeld number Vs Eccentricity ratio for different L/D ratio

The plot shows the relationship between the Sommerfeld number and the eccentricity ratio for journal bearings with different Length-to-Diameter (L/) ratios (L/D = 1, L/D = 0.5, L/D = 0.25). facilitating a comparison between our results and those documented in the table 3.

Analyzing the graph, we observe distinct trends for each L/D ratio:

- **L/D = 1 (Blue Line)**: The Sommerfeld number decreases gradually as the eccentricity ratio increases. This indicates that bearings with a higher L/D ratio (i.e., longer bearings relative to their diameter) maintain a more stable operation with minimal load impact at higher eccentricities.
- **L/D = 0.5 (Orange Line)**: The trend is similar to the L/D = 1 case but with a sharper decline in the Sommerfeld number as the eccentricity ratio increases. This suggests that the bearing's load-bearing capacity reduces more significantly as eccentricity changes.
- **L/D = 0.25 (Grey Line)**: Shows a steep decline in Sommerfeld number with an increase in the eccentricity ratio. This indicates that bearings with a low L/D ratio (shorter bearings) are more sensitive to changes in eccentricity, implying a lower load-bearing capacity and reduced operational stability.

In summary, the graph reveals that as the L/D ratio decreases, the bearing's sensitivity to changes in eccentricity increases, leading to a more significant reduction in the Sommerfeld number. This means that bearings with lower L/D ratios are less stable and more affected by varying operational conditions, particularly at higher eccentricity ratios.

5.2.2 Results and plotting of Journal Position in the Hydrodynamic Bearing throughout the cycle:

Here we have plotted the graph for Journal center position or journal displacement and attitude angle against crank angles.

The graph plots the journal displacement in millimeters against the crank angle in degrees for Bearing 1.

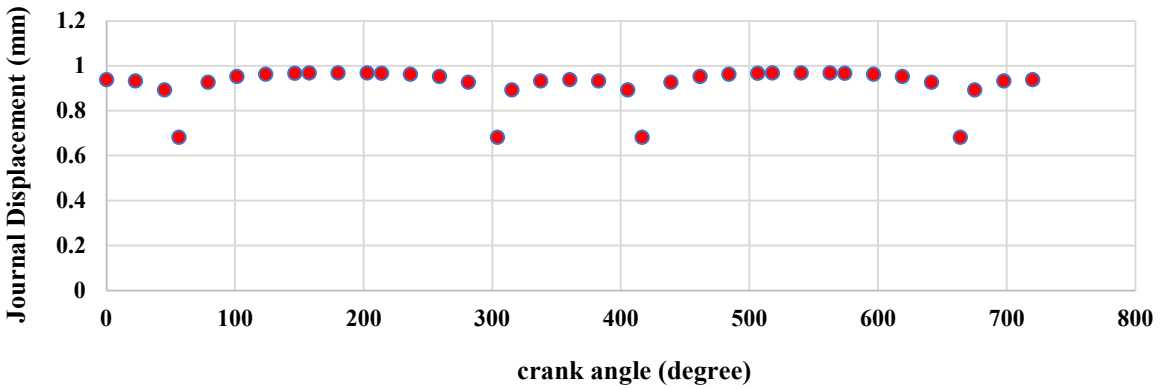

Figure 16. Journal displacement (eccentricity) VS crank angle for Bearing_1

The journal displacement fluctuates slightly around 0.8 to 1.0 mm, with a few outliers at certain crank angles where the displacement deviates more significantly.

The journal maintains a relatively stable position with minor fluctuations throughout the engine cycle, indicating consistent load distribution on bearing 1. Occasional drops in displacement suggest transient forces acting on the journal, possibly due to changes in engine speed or load.

The graph suggests that the journal maintains a relatively stable position within the bearing throughout the crank cycle, with minimal variation. However, the slight dips indicate moments of reduced lubrication film thickness, which could lead to potential contact or wear at those points.

This graph illustrates how the attitude angle (in degree) varies with the crank angle for bearing_1.

The variation in the attitude angle suggests dynamic changes in the hydrodynamic pressure distribution within the bearing during the engine cycle.

Peaks in the attitude angle could be associated with moments of increased load or misalignment, affecting the stability of the bearing.

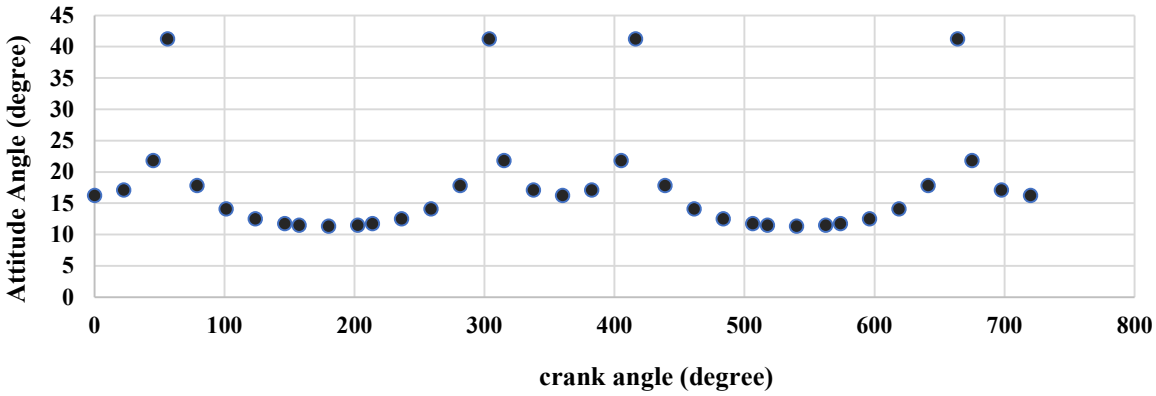

Figure 17. Attitude angle VS crank angle For Bearing_1

The varying attitude angle suggests that the alignment of the journal within the bearing changes dynamically throughout the engine cycle. Higher attitude angles may correspond to moments of increased load or misalignment, which could impact the bearing's performance and longevity.

In the similar manner following graph for bearing 2 can be explained.

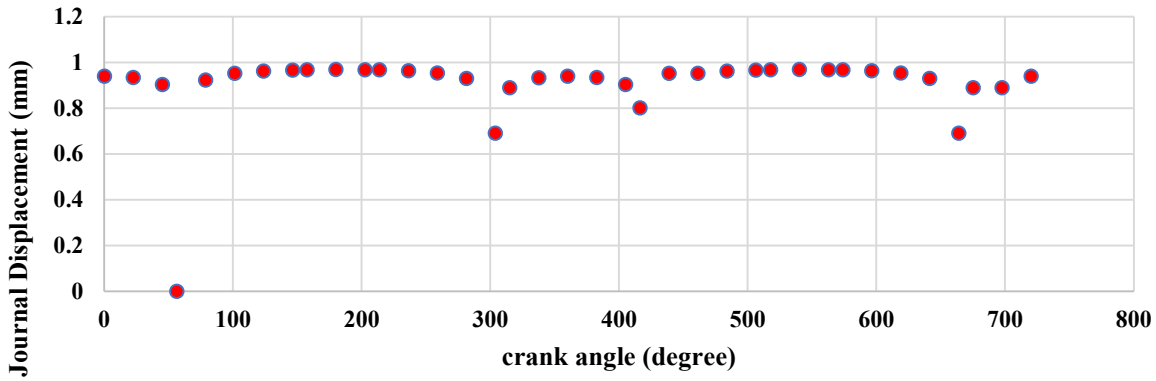

Figure 18. Journal displacement (eccentricity) VS crank angle for Bearing_2

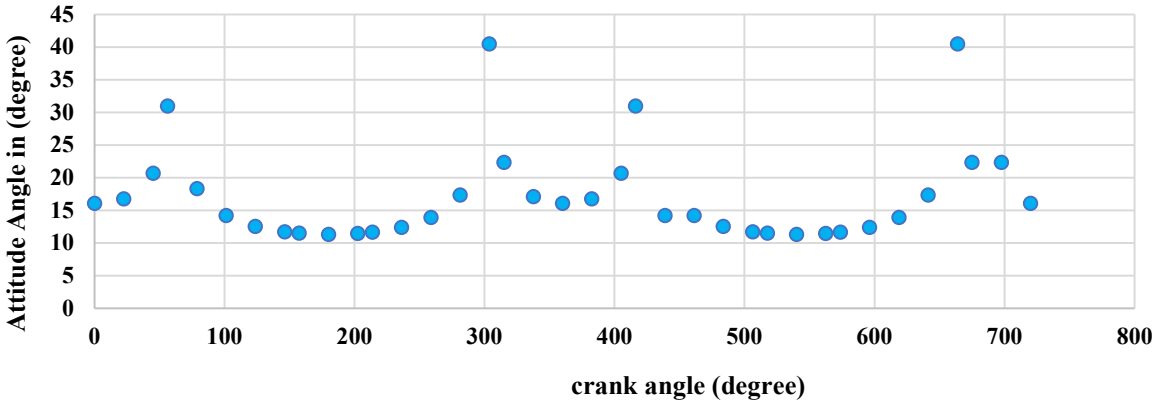

Figure 19. Attitude angle VS crank angle For Bearing_2

The overall interpretation from the above plots for bearing 1 & bearing 2 are bearing 1 generally shows more stability in both journal position and attitude angle compared to bearing 2, which experiences greater fluctuations.

The fluctuations in the attitude angle for bearing 2 suggest more dynamic changes in load distribution, which could affect the longevity and performance of the bearing.

This analysis highlights the importance of monitoring both the journal position and attitude angle to assess the performance and stability of journal bearings in IC engines.

5.3 Comparison with Theoretical and Experimental Data

Validation of the Results with the Chart for determining the position of the minimum film thickness h_0. (Raimondi and Boyd.)

The data from our Bearing Consideration -

epsilon = 0.5
phi = 0
epsilon_dot = 0
phi_dot = 0
omega = 2000np.pi
Ld = 1
Bearing_clearence=0.001 m
Bearing_radius=0.026 m
miu=0.025 pa-sec
Atmospheric_pressure=101325 pa
spacing = Ld/20
min_relative_error=1e-4
relaxation_coefficient=0.3
max_iterations=3000
absolute_error_force=0.1
relative_error_force=0.01
Bearing_force0 = 50661.8387601943 N

The output we get-

Bearing Number = 6.287836073506144
Sommerfeld Number = 0.0008339610451169881
Dimensionless Bearing Force = 176.4443223453639
Reference Force = 287.12648889336987 N
Bearing Force = 50661.8387601943 N
Attitude angle = 11.309119866152896 degrees
Iteration completed = 2999 Numbers
RMSE of Relative error of pressure estimation = 0.00
4387831641899484
Optimization terminated successfully.

Eccentricity found at: [0.96856384]

Thus, given the range of eccentricity values, we can determine the minimum fluid film thickness. In this scenario we have identified the maximum eccentricity observed for bearing_2, and the maximum eccentricity occurs at a crank angle of 180 degrees, measuring 0.96856384 with an attitude angle of 11.30912 degree, while maintaining a clearance of 1mm.

We have minimum film thickness, $h_0 = c(1 - \varepsilon)$

or, $h_0 = 0.03143616\ mm$

Now we can validate our calculation from Raimondi and Boyd chart for determining the position of the minimum film thickness h_0. (Chart reference – [2] Shigley's Mechanical Engineering Design-Lubrication and Journal Bearings- Figure 12–16 Chart for determining the position of the minimum film thickness h_0. (figure 20))

Chapter 6

Conclusion and Future Work

6.1 Summary of Findings

This thesis presents a comprehensive study on the dynamic analysis of journal bearings within a Single Cylinder Four-Stroke Engine model, focusing on pressure distribution, Sommerfeld number, journal position, and attitude angle throughout the engine cycle. The project employs both analytical and numerical methods, such as the Finite Difference Method (FDM) to solve the Reynolds equation under the Half-Sommerfeld boundary condition, providing an in-depth examination of the hydrodynamic lubrication behavior in journal bearings.

The analysis of pressure distribution reveals the critical role of high-pressure regions in supporting the load carried by the bearing, with significant variations depending on the eccentricity ratio and the bearing's length-to-diameter (L/D) ratio. The study highlights that bearings with higher L/D ratios exhibit greater stability, maintaining more consistent load-carrying capacity even as the eccentricity ratio increases. Conversely, bearings with lower L/D ratios demonstrate heightened sensitivity to changes in eccentricity, resulting in a sharper decline in the Sommerfeld number and reduced operational stability.

Furthermore, the investigation into journal position and attitude angle shows that while bearing 1 generally maintains a stable position with minor fluctuations, bearing 2 experiences greater instability, as evidenced by more significant variations in both journal displacement and attitude angle. These findings underscore the importance of monitoring these parameters to ensure optimal bearing performance and longevity.

The thesis also validates the computational results against established theoretical models, such as Raimondi and Boyd’s charts for determining minimum fluid film thickness, confirming the accuracy and reliability of the methods used.

In conclusion, this project delves into the dynamic analysis of a Single Cylinder Four-Stroke Engine model, focusing on understanding the complex interactions between piston motions, pressure distribution, and bearing reaction forces. Through analytical and numerical methods, we have investigated the behavior of the engine’s components throughout a complete cycle, offering valuable insights into key aspects such as bearing reactions and journal position.

6.2 Limitations of the Study

By assuming linear characteristics of piston pressure and employing the relaxation method of Finite Element Method (FEM), we have successfully determined the journal position for a finite length bearing. The Python code developed for this purpose provides a versatile tool for predicting journal positions under different operating conditions, facilitating optimization efforts for engine performance and reliability.

6.3 Contributions to the Field

The findings of this project contribute valuable insights into engine dynamics and offer practical implications for optimizing internal combustion engines. Understanding the forces experienced by bearings and accurately predicting journal positions are crucial steps towards enhancing engine performance, durability, and efficiency.

Moreover, the methodologies developed and the insights gained lay the groundwork for future research and optimization efforts. Further exploration could involve refining the modelling techniques, experimental validation, and extending the analysis to more complex engine configurations.

6.4 Recommendations for Future Research

Future research on journal bearings in single-cylinder four-stroke IC engines should focus on several key areas. Exploring advanced lubrication models that consider non-Newtonian fluids and thermal effects could enhance simulation accuracy. Incorporating dynamic load conditions and validating numerical results with experimental data will improve the realism and reliability of the findings. Investigating alternative materials for wear resistance, optimizing design parameters, and analyzing the impact of alternative fuels are also essential. Additionally, future studies could examine environmental factors and integrate bearing performance simulations with engine control systems to optimize efficiency and durability. These areas of research would advance the understanding and application of journal bearings in IC engines, contributing to more efficient and reliable engine designs.

Chapter 7

References

7.1 List of all references used in the thesis

[1] Bhandari, V.B.,"Design of Machine Elements, 3e", McGraw-Hill Education – Europe, Ch – 25, pp – 880-903

[2] Richard G. Budynas, J. Keith Nisbett, Kiatfa Tangchaichit, "Shigley'S Mechanical Engineering Design (SIE)", Chapter 12: Lubrication and Journal Bearings, McGraw Hill; Eleventh edition (5 November 2020), Ch – 12, pp - 640-642

[3] Chasalevris, A. and Sfyris, D., 2013. Evaluation of the finite journal bearing characteristics, using the exact analytical solution of the Reynolds equation. *Tribology International*, *57*, pp.216-234.

[4] Suryawanshi, S.R. and Pattiwar, J.T., 2016. An Overview on Theoretical Analysis of Hydrodynamic Journal Bearing Considering Thermal Effects. International Journal of Machine Design and Manufacturing, 1(2), pp.45-57.

[5] Machado, T.H., Alves, D.S. and Cavalca, K.L., 2018. Discussion about nonlinear boundaries for hydrodynamic forces in journal bearing. *Nonlinear Dynamics*, *92*, pp.2005-2022.

[6] Liang, P., Lu, C., Ding, J. and Chen, S., 2013. A method for measuring the hydrodynamic effect on the bearing land. *Tribology International*, *67*, pp.146-153.

[7] Najar, F.A. and Harmain, G.A., 2014. Numerical investigation of pressure profile in hydrodynamic lubrication thrust bearing. International scholarly research notices, 2014(1), p.157615.

[8] Sharma, R.K. and Pandey, R.K., 2009. Experimental studies of pressure distributions in finite slider bearing with single continuous surface profiles on the pads. *Tribology International*, *42*(7), pp.1040-1045.

[9] Zhang, C., Wang, S. and Zhang, Y., 2015, August. Pressure distribution analysis of elastohydrodynamic journal bearing under grease lubrication. In *2015 International Conference on Fluid Power and Mechatronics (FPM)* (pp. 74-79). IEEE.

[10] Yoshimoto, S., Yamamoto, M. and Toda, K., 2007. Numerical calculations of pressure distribution in the bearing clearance of circular aerostatic thrust bearings with a single air supply inlet.

[11] Karmakar, Mintu & Tudu, Suplal & Sarkar, Susenjit & Mondal, Samar. (2020). COMPARISON OF ERRORS IN CALCULATING THE JOURNAL FORCE OF A SHORT CYLINDRICAL OIL FILM BEARING. 59-63. 10.26480/cic.01.2020.59.63.

[12] Meng, F. and Chen, Y., 2015. Analysis of elasto-hydrodynamic lubrication of journal bearing based on different numerical methods. *Industrial Lubrication and Tribology*, *67*(5), pp.486-497.

[13] Failawati, V., Yamin, M., Poernomosari, S. and Naik, A.R., 2022. CFD Analysis of the Eccentricity Ratio on Journal Bearing due to Differences in Lubrication Type. *Journal of Novel Engineering Science and Technology*, *1*(02), pp.51-56.

[14] Huang, P. 2013). Numerical Calculation of Lubrication Methods and Programs, Wiley, Singapore, 12-101

Chapter 8
Appendices

8.1 Detailed Code (In Python)

```
import numpy as np
import math
import time
from scipy.optimize import fmin
import matplotlib.pyplot as plt
#from mpl toolkits.mplot3d import Axes3D

def create square grid(length, width, spacing):
    i = np.arange(0, length + spacing, spacing)
    alpha = np.arange(0, width + spacing, spacing)
    grid i, grid alpha = np.meshgrid(i, alpha)
    return grid i, grid alpha

def calculate coefficients(epsilon, phi, epsilon dot, phi dot, omega, theta,
spacing):
    H = 1 - epsilon * np.cos(theta - phi)
    Hip=1 - epsilon * np.cos(theta+0.5*spacing - phi)
    Him=1 - epsilon * np.cos(theta-0.5*spacing - phi)
    A = (Hip[:-1] ** 3)
    B = (H[:-1] ** 3)
    D = (Him[1:] ** 3)
    C = -(A + D + 2 * B)
    E = B
    F = spacing ** 2 * (epsilon * np.sin(theta - phi) - (2/omega) * (epsilon * phi
dot * np.sin(theta - phi) + epsilon dot * np.cos(theta - phi)))
    return A, B, C, D, E, F, H, Hip, Him

def conventional FDM iteration with boundary conditions(P, A, B, C, D, E, F, max
iterations, relaxation coefficient, min relative error):

    # Apply initiation
    P[:, :]=0.5

    # Apply boundary conditions
    P[0,:] = 0  # Set first row to 0
    P[-1,:] = 0  # Set last row to 0
    P[:, 0] = 0  # Set first column to 0
    P[:, -1] = 0  # Set last column to 0



    for iteration in range(max iterations):
```

```
        P previous = P.copy()
        for i in range(1, len(P)-1):
            for j in range(1, len(P[i])-1):
                P[i, j] = (F[i, j] - A[i, j] * P[i-1, j] - B[i, j-1] * P[i, j-1] -
D[i, j] * P[i+1, j] - E[i, j+1] * P[i, j+1]) / C[i, j]

        # Apply boundary conditions
        P[0,:] = 0  # Set first row to 0
        P[-1,:] = 0  # Set last row to 0
        P[:, 0] = 0  # Set first column to 0
        P[:, -1] = 0  # Set last column to 0

        # Apply relaxation coefficients
        P = relaxation coefficient * P + (1-relaxation coefficient) * P previous

        # Check for convergence
        relative error = np.where(np.logical or(np.abs(P) < 0.00000001, np.abs(P
previous) < 0.00000001),
                          0,
                          ((P - P previous) / np.maximum(np.abs(np.maximum(P
previous, P)), 0.0001))).astype(np.float64)  # Cast to float64  to Avoid divide by
zero
        relative error = np.nan to num(relative error)  # Replace NaN with zero
        #relative error = np.abs((P - P previous) / np.maximum(P previous,
P)).astype(np.float64)  # Cast to float64
        rmse relative error = np.sqrt(np.mean(relative error ** 2))

        max value = np.max(np.abs(relative error))
        if max value > 1:
            relative error /= max value  # Scale to values between -1 and 1
            rmse relative error = np.sqrt(np.mean(relative error ** 2)) * max value
# Rescale RMSE

        if rmse relative error < min relative error:
            break
    return P, iteration, rmse relative error

def simulate pressure distribution(epsilon, phi, epsilon dot, phi dot, omega, Ld,
spacing,max iterations, relaxation coefficient, min relative error):
    # Create square grid
    spacing i=spacing
    spacing alpha=spacing
    theta, z = create square grid(2 * np.pi, 2*Ld, spacing i)

    # Calculate coefficients and simulate pressure distribution
    A, B, C, D, E, F, H, Hip, Him= calculate coefficients(epsilon, phi, epsilon
dot, phi dot, omega, theta, spacing alpha)
    P initial = np.zeros like(theta)  # Initial guess for pressure
```

```
    P solution, iteration, rmse relative error = conventional FDM iteration with
boundary conditions(
        P initial, A, B, C, D, E, F, max iterations, relaxation coefficient, min
relative error
    )
    P solution filtered = [[max(0, value) for value in row] for row in P solution]

# Considering half sommerfield condition
    P solution filtered = np.array(P solution filtered).reshape(theta.shape)
    return theta, z, P solution, P solution filtered,iteration, rmse relative error

def calculate bearing force(epsilon, phi, epsilon dot, phi dot, omega, Ld, Bearing
clearence, Bearing radius, miu, Atmospheric pressure, spacing, min relative error,
relaxation coefficient, max iterations,plotflag):

  """
  Calculates the bearing force and Sommerfeld number for a journal bearing.

  Args:
    epsilon: Eccentricity ratio.
    phi: Phase angle.
    epsilon dot: Rate of change of eccentricity ratio.
    phi dot: Rate of change of phase angle.
    omega: Shaft rotational speed (rad/s).
    Ld: Bearing length to Diameter ratio.
    Bearing clearence: Bearing clearance (m).
    Bearing radius: Bearing radius (m).
    miu: Dynamic viscosity of the lubricant (Pa·s).
    Atmospheric pressure: Atmospheric pressure (Pa).
    spacing: Dimensionless Grid spacing for pressure calculation.
    min relative error: Minimum relative error for pressure convergence.
    relaxation coefficient: Relaxation coefficient for pressure calculation.
    max iterations: Maximum number of iterations for pressure calculation.
    plotflag = 1 for ploting o for not ploting

  Returns:
    Bearing number: Bearing number (dimensionless).
    Sm: Sommerfeld number (dimensionless).
    Bearing force: Bearing force magnitude (N).
  """

  # Calculate bearing number
  Bearing number = 6 * miu * omega * Bearing radius * Bearing radius / (Atmospheric
pressure * Bearing clearence ** 2)



# Simulate pressure distribution
```

```
  theta, z, P solution, P solution filtered,iteration, rmse relative error =
simulate pressure distribution(epsilon, phi, epsilon dot, phi dot, omega, Ld,
spacing, max iterations, relaxation coefficient, min relative error)

# Calculate force components from pressure distribution
  F x, F y = 0, 0
  for i in range(theta.shape[0]):
    for j in range(theta.shape[1]):
      if P solution filtered[i][j] > 0:
        F x += P solution filtered[i][j] * spacing ** 2 * np.cos(theta[i, j])
        F y += P solution filtered[i][j] * spacing ** 2 * np.sin(theta[i, j])

  # Calculate bearing force magnitude
  Bearing force= Atmospheric pressure*Bearing radius*Bearing radius*Bearing
number*np.sqrt(F x**2+F y**2)

  # Calculate Sommerfeld number
  Sm = (0.5 / np.pi) * (((Bearing radius - Bearing clearence) / Bearing clearence)
** 2) * miu * omega * Ld * 4 * Bearing radius * Bearing radius / Bearing force
  attitude angle=math.degrees(math.atan(-F y/F x))
  F reference=(miu*omega*Bearing radius*(Ld*2*Bearing radius)**3)/(2*Bearing
clearence**2)
  Dimensionless Bearing force=Bearing force/F reference

  # Print calculated values
  print(f"Bearing Number = {Bearing number}")
  print(f"Sommerfeld Number = {Sm}")
  print(f"Dimensionless Bearing Force = {Dimensionless Bearing force}")
  print(f"Reference Force = {F reference} N")
  print(f"Bearing Force = {Bearing force} N")
  print(f"Attitude angle = {attitude angle} degrees")
  print(f"Iteration completed = {iteration} Numbers")
  print(f"RMSE of Relative error of pressure estimation = {rmse relative error}")

  if plotflag==1:
    plot pressure distribution(theta, z, P solution filtered)

  # Return calculated values
  return Bearing number, Sm, Bearing force, Dimensionless Bearing force, F
reference, attitude angle, theta, z, P solution, P solution filtered,iteration,
rmse relative error

def plot pressure distribution(theta, z, P solution filtered, title="Dimensionless
excess pressure distribution", cmap="jet", aspect="auto"):
  """
  Creates a 3D surface plot of the dimensionless excess pressure distribution on a
bearing surface.
```

```
  Args:
    theta: Array of angular coordinates (radians).
    z: Array of axial coordinates (normalized).
    P solution filtered: Array of dimensionless excess pressure values.
    title: Optional title for the plot (default: "Dimensionless excess pressure
distribution").
    cmap: Optional colormap for the surface plot (default: "jet").
    aspect: Optional aspect ratio for the plot axes (default: "auto").

  Returns:
    None (the plot is displayed directly).
  """

  # Create a figure and 3D subplot
  fig = plt.figure()
  ax = fig.add subplot(111, projection="3d", **{'aspect': aspect})

  # Plot the surface
  surface = ax.plot surface(theta, z, P solution filtered, cmap=cmap)

  # Add labels and title
  ax.set xlabel("Theta")
  ax.set ylabel("Z")
  ax.set zlabel("Dimensionless excess pressure")
  ax.set title(title)

  # Add a colorbar
  fig.colorbar(surface, ax=ax, shrink=0.5, aspect=10)

  # Show the plot
  plt.show()

def error correction(absolute error, relative error, total time resource, data,
function to correct, *args, **kwargs):
    # 1. Initialize variables
    error = data+absolute error*(1+np.abs(relative error))  # Measure initial error
    args list = list(args)  # Create a mutable copy
    newspace=args list[10]
    newiteration=args list[13]
    start time = time.time()
    # 2. Iteration loop
    while np.any(error > absolute error) or np.any(error / data > relative error):

        if time.time() - start time > 1+total time resource:
            plot pressure distribution(theta, z, P solution filtered,
title="Dimensionless excess pressure distribution", cmap="jet", aspect="auto")
            raise TimeoutError("Exceeded computation time limit")
        else:
```

```
            # 3. Perform error correction step
            newspace = 1.0 * newspace  # Modify the 10th element
            newiteration = int(1.5 * newiteration)  # Modify the 13th element
            args list[10]=newspace
            args list[13]=newiteration
            Bearing number, Sm, Bearing force, Dimensionless Bearing force, F
reference, attitude angle, theta, z, P solution, P solution filtered,iteration,
rmse relative error = correction step(data, function to correct, *args list,
**kwargs)
            corrected data=Bearing force
            # 4. Update error and data
            error = calculate error(corrected data, data)  # Assuming a present
data is reference exists
            data = corrected data
            print(f"Absolute error of Force = {error} N")
            print(f"Relative error of Force = {error / data}")
            print(f"Time lapsed for error correction = {(time.time() - start
time)}")
    # 5. Return corrected data
    return Bearing number, Sm, Bearing force, Dimensionless Bearing force, F
reference, attitude angle, theta, z, P solution, P solution filtered,iteration,
rmse relative error

def correction step(data, function to correct, *args, **kwargs):
    """Applies the given correction function to the data."""
    Bearing number, Sm, Bearing force, Dimensionless Bearing force, F reference,
attitude angle, theta, z, P solution, P solution filtered,iteration, rmse relative
error = function to correct(*args, **kwargs)
    #corrected data=Bearing force
    return Bearing number, Sm, Bearing force, Dimensionless Bearing force, F
reference, attitude angle, theta, z, P solution, P solution filtered,iteration,
rmse relative error

def calculate error(corrected data, reference data):
    """ Error calculation logic here."""
    corrected data = np.array(corrected data)
    reference data = np.array(reference data)
    return np.abs(corrected data - reference data)


# Example usage also validated with
http://dx.doi.org/10.1016/j.triboint.2012.08.011


epsilon = 0.5
phi = 0
epsilon dot = 0
phi dot = 0
```

```
omega = 2000*np.pi
Ld = 1
Bearing clearence=0.001
Bearing radius=0.026
miu=0.025
Atmospheric pressure=101325
spacing = Ld/20
min relative error=1e-4
relaxation coefficient=0.3
max iterations=3000

absolute error force=0.1
relative error force=0.01
total time resource=60
flag=0
Bearing force0=50660.27792

def my function(x, Bearing force0, phi, epsilon dot, phi dot, omega, Ld, Bearing
clearence, Bearing radius, miu, Atmospheric pressure, spacing, min relative error,
relaxation coefficient, max iterations, flag):
    # Your function to minimize here
    Bearing number, Sm, Bearing force, Dimensionless Bearing force, F reference,
attitude angle, theta, z, P solution, P solution filtered, iteration, rmse relative
error = calculate bearing force(x, phi, epsilon dot, phi dot, omega, Ld, Bearing
clearence, Bearing radius, miu, Atmospheric pressure, spacing, min relative error,
relaxation coefficient, max iterations, flag)

    return np.abs(Bearing force0 - Bearing force)

# Initial guess for the minimum
x0 = np.array([0.5])

# Find the minimum
x min= fmin(my function, x0, args=(Bearing force0, phi, epsilon dot, phi dot,
omega, Ld, Bearing clearence, Bearing radius, miu, Atmospheric pressure, spacing,
min relative error, relaxation coefficient, max iterations, flag),xtol=0.02,
ftol=1, maxiter=None, maxfun=None, full output=0, disp=1, retall=0, callback=None,
initial simplex=None)

print("Eccentricity found at:", x min)
```

Output for 180-degree crank position with 50660.27792 N Bearing Force for bearing 2:

Bearing Number = 6.287836073506144
Sommerfeld Number = 0.0004170027621063902
Dimensionless Bearing Force = 1411.479297881068
Reference Force = 35.89081111167123 N
Bearing Force = 50659.13686828375 N
Attitude angle = 6.909159960766361 degrees
Iteration completed = 2999 Numbers
RMSE of Relative error of pressure estimation = 0.010559193797776626
Optimization terminated successfully.
    Current function value: 1.141052
    Iterations: 25
    Function evaluations: 50
Eccentricity found at: [0.98729973]

In summary, this code provides a tool for determining the required eccentricity to achieve a specific bearing force under given operating conditions for a journal bearing with an L/D ratio of 1, but also, we can find the results for different values of Operating speeds and L/D ratio.

8.2 Additional Graphs and Tables

The output values in a tabular format for better understanding and reference.

Table 1. Results for P_p, $(R_1)_v$, $(R_1)_h$ & Resultant Reaction on bearing 1 & 2

SL. NO.	Theata (radian)	Theata (degree)	Force exerted on piston P_p	$(R_1)_v$	$(R_1)_v$	Resultant Reaction on bearing 1 (R_1) [in N]	Resultant Reaction on bearing 2 (R_2) [in N]
1	0	0	30679.615	15339.8075	0	15339.8075	15871.34215
2	0.196349541	11.25	29421.23889	14303.42201	3495.989283	14724.4634	15471.1093
3	0.392699082	22.5	25694.46923	11449.68061	5929.467698	12893.94327	13813.48577
4	0.589048623	33.75	19642.52371	7487.239826	6472.358032	9896.978262	10937.64758
5	0.785398163	44.99999999	11497.97519	3418.336475	4711.959752	5821.304747	6926.748511
6	0.981747704	56.24999999	1573.814101	314.1703627	736.4831378	800.6937174	1917.875665
7	1.178097245	67.49999999	-9748.579608	-920.6381527	-4894.552457	4980.383355	3917.202483
8	1.374446786	78.74999999	-22034.0927	263.7445348	-11285.3451	11288.4266	10313.66227
9	1.570796327	89.99999999	-34810.59979	3967.036019	-17405.2999	17851.66209	17002.59614
10	1.767145868	101.25	-47587.10688	9853.393998	-22299.73478	24379.65432	23682.72512
11	1.963495408	112.5	-59872.61997	17257.99823	-25254.33151	30587.90223	30060.25778
12	2.159844949	123.75	-71195.01368	25341.62875	-25880.02247	36221.17766	35872.06845
13	2.35619449	135	-81119.17477	33243.26939	-24116.64918	41069.79093	40902.17229
14	2.552544031	146.25	-89263.72329	40194.96981	-20179.20511	44975.9482	44988.02592
15	2.748893572	157.5	-95315.66881	45586.69844	-14479.89722	47831.10387	48017.61554
16	2.945243113	168.75	-99042.43847	48988.9191	-7553.467871	49567.82294	49920.94805
17	3.141592654	180	-100300.8146	50150.40729	2.98654E-11	50150.40729	50660.27792
18	3.337942194	191.25	-99042.43847	48988.9191	7553.467871	49567.82294	50222.65351
19	3.534291735	202.5	-95315.66881	45586.69844	14479.89722	47831.10387	48616.98253
20	3.730641276	213.75	-89263.72329	40194.96981	20179.20511	44975.9482	45876.3479
21	3.926990817	225	-81119.17477	33243.26939	24116.64918	41069.79093	42064.88197
22	4.123340358	236.25	-71195.01368	25341.62875	25880.02247	36221.17766	37287.06726
23	4.319689899	247.5	-59872.61997	17257.99823	25254.33151	30587.90223	31696.00013
24	4.51603944	258.75	-47587.10688	9853.393998	22299.73478	24379.65432	25496.47835
25	4.71238898	270	-34810.59979	3967.036019	17405.29989	17851.66209	18939.62711
26	4.908738521	281.25	-22034.0927	263.7445348	11285.3451	11288.4266	12309.0621
27	5.105088062	292.5	-9748.579608	-920.6381527	4894.552457	4980.383355	5909.541871

28	5.301437603	303.75	1573.814101	314.1703627	-736.4831378	800.6937174	855.7537707
29	5.497787144	315	11497.97519	3418.336475	-4711.959752	5821.304747	5397.407334
30	5.694136685	326.25	19642.52371	7487.239826	-6472.358032	9896.978262	9682.081515
31	5.890486225	337.5	25694.46923	11449.68061	-5929.467698	12893.94327	12926.50449
32	6.086835766	348.75	29421.23889	14303.42201	-3495.989283	14724.4634	15012.37042
33	6.283185307	360	30679.615	15339.8075	7.86668E-11	15339.8075	15871.34215
34	6.479534848	371.25	29421.23889	14303.42201	3495.989283	14724.4634	15471.1093
35	6.675884389	382.5	25694.46923	11449.68061	5929.467698	12893.94327	13813.48577
36	6.87223393	393.7499999	19642.52371	7487.239826	6472.358032	9896.978262	10937.64758
37	7.068583471	404.9999999	11497.97519	3418.336475	4711.959752	5821.304747	6926.748511
38	7.264933011	416.2499999	1573.814101	314.1703627	736.4831378	800.6937174	1917.875665
39	7.461282552	427.4999999	-9748.579608	-920.6381527	-4894.552457	4980.383355	3917.202483
40	7.657632093	438.7499999	-22034.0927	263.7445348	-11285.3451	11288.4266	10313.66227
41	7.853981634	449.9999999	-34810.59979	3967.036019	-17405.2999	17851.66209	17002.59614
42	8.050331175	461.2499999	-47587.10688	9853.393998	-22299.73478	24379.65432	23682.72512
43	8.246680716	472.4999999	-59872.61997	17257.99823	-25254.33151	30587.90223	30060.25778
44	8.443030257	483.7499999	-71195.01368	25341.62875	-25880.02247	36221.17766	35872.06845
45	8.639379797	494.9999999	-81119.17477	33243.26939	-24116.64918	41069.79093	40902.17229
46	8.835729338	506.2499999	-89263.72329	40194.96981	-20179.20511	44975.9482	44988.02592
47	9.032078879	517.4999999	-95315.66881	45586.69844	-14479.89722	47831.10387	48017.61554
48	9.22842842	528.7499999	-99042.43847	48988.9191	-7553.467871	49567.82294	49920.94805
49	9.424777961	539.9999999	-100300.8146	50150.40729	5.4952E-11	50150.40729	50660.27792
50	9.621127502	551.2499999	-99042.43847	48988.9191	7553.467871	49567.82294	50222.65351
51	9.817477042	562.4999999	-95315.66881	45586.69844	14479.89722	47831.10387	48616.98253
52	10.01382658	573.7499999	-89263.72329	40194.96981	20179.20511	44975.9482	45876.3479
53	10.21017612	584.9999999	-81119.17477	33243.26939	24116.64918	41069.79093	42064.88197
54	10.40652567	596.2499999	-71195.01368	25341.62875	25880.02247	36221.17766	37287.06726
55	10.60287521	607.4999999	-59872.61997	17257.99823	25254.33151	30587.90223	31696.00013
56	10.79922475	618.7499999	-47587.10688	9853.393998	22299.73478	24379.65432	25496.47835
57	10.99557429	629.9999999	-34810.59979	3967.036019	17405.2999	17851.66209	18939.62711
58	11.19192383	641.2499999	-22034.0927	263.7445348	11285.3451	11288.4266	12309.0621
59	11.38827337	652.4999999	-9748.579608	-920.6381527	4894.552457	4980.383355	5909.541871
60	11.58462291	663.7499999	1573.814101	314.1703627	-736.4831378	800.6937174	855.7537707

61	11.78097245	674.9999999	11497.97519	3418.336475	-4711.959752	5821.304747	5397.407334
62	11.97732199	686.2499999	19642.52371	7487.239826	-6472.358032	9896.978262	9682.081515
63	12.17367153	697.4999999	25694.46923	11449.68061	-5929.467698	12893.94327	12926.50449
64	12.37002107	708.7499999	29421.23889	14303.42201	-3495.989283	14724.4634	15012.37042
65	12.56637061	719.9999999	30679.615	15339.8075	-1.75709E-10	15339.8075	15871.34215

Table 2. Results for Journal position (eccentricity and attitude angle) for complete cycle

Resultant Reaction on bearing 1 (R_1) [in N]	Journal position (Ecentricity) for bearing 1 [in mm]	Journal position (Attitude Angle) for bearing 1 [in degree]	Resultant Reaction on bearing 2 (R_2) [in N]	Journal position (Ecentricity) for bearing 2 [in mm]	Journal position (Attitude Angle) for bearing 2 [in degree]
15339.8075	0.93829346	16.2207	15871.34215	0.93946533	16.0538
14724.4634			15471.1093		
12893.94327	0.93193359	17.1046	13813.48577	0.9345214	16.7469
9896.978262			10937.64758		
5821.304747	0.89321289	21.8307	6926.748511	0.9031982	20.6896
800.6937174	0.68125	41.2654	1917.875665	0.80117188]	30.98359
4980.383355			3917.202483		
11288.4266	0.92657471	17.8105	10313.66227	0.92272339	18.30887
17851.66209			17002.59614		
24379.65432	0.95252686	14.0952	23682.72512	0.9517334	14.21788
30587.90223			30060.25778		
36221.17766	0.96203156	12.5085	35872.06845	0.96182556	12.54474
41069.79093			40902.17229		
44975.9482	0.9663887	11.7204	44988.02592	0.96640625	11.7217
47831.10387	0.9675354	11.5052	48017.61554	0.96760406	11.49229
49567.82294			49920.94805		
50150.40729	0.96838455	11.3436	50660.27792	0.96856384	11.30911
49567.82294			50222.65351		
47831.10387	0.9675354	11.5052	48616.98253	0.96783447	11.44859
44975.9482	0.9663887	11.7204	45876.3479	0.96676025	11.65056
41069.79093			42064.88197		
36221.17766	0.96203156	12.5085	37287.06726	0.96264801	12.399839
30587.90223			31696.00013		
24379.65432	0.95252686	14.0952	25496.47835	0.95371094	13.905143
17851.66209			18939.62711		
11288.4266	0.92657471	17.8105	12309.0621	0.93009033	17.34576
4980.383355			5909.541871		
800.6937174	0.68125	41.2654	855.7537707	0.690625	40.47436
5821.304747	0.89321289	21.8307	5397.407334	0.88857422	22.34653
9896.978262			9682.081515		
12893.94327	0.93193359	17.1046	12926.50449	0.93203125	17.091438
14724.4634			15012.37042		
15339.8075	0.93829346	16.2207	15871.34215	0.93946533	16.053818
14724.4634			15471.1093		
12893.94327	0.93193359	17.1046	13813.48577	0.93452148	16.746928
9896.978262			10937.64758		
5821.304747	0.89321289	21.8307	6926.748511	0.90319824	20.689636
800.6937174	0.68125	41.2654	1917.875665	0.80117188	30.983593

4980.383355			3917.202483		
11288.4266	0.92657471	17.8105	10313.66227	0.9517334	14.21788915
17851.66209			17002.59614		
24379.65432	0.95252686	14.0952	23682.72512	0.9517334	14.21788
30587.90223			30060.25778		
36221.17766	0.96203156	12.5085	35872.06845	0.96182556	12.54474
41069.79093			40902.17229		
44975.9482	0.9663887	11.7204	44988.02592	0.96640625	11.7217
47831.10387	0.9675354	11.5052	48017.61554	0.96760406	11.49229
49567.82294			49920.94805		
50150.40729	0.96838455	11.3436	50660.27792	0.96856384	11.30911
49567.82294			50222.65351		
47831.10387	0.9675354	11.5052	48616.98253	0.96783447	11.44859
44975.9482	0.9663887	11.7204	45876.3479	0.96676025	11.65056
41069.79093			42064.88197		
36221.17766	0.96203156	12.5085	37287.06726	0.96264801	12.399839
30587.90223			31696.00013		
24379.65432	0.95252686	14.0952	25496.47835	0.95371094	13.905143
17851.66209			18939.62711		
11288.4266	0.92657471	17.8105	12309.0621	0.93009033	17.34576
4980.383355			5909.541871		
800.6937174	0.68125	41.2654	855.7537707	0.690625	40.47436
5821.304747	0.89321289	21.8307	5397.407334	0.88857422	22.34653
9896.978262			9682.081515		
12893.94327	0.93193359	17.1046	12926.50449	0.88857422	22.34653
14724.4634			15012.37042		
15339.8075	0.93829346	16.2207	15871.34215	0.93946533	16.0538

Table 3. Variation in parameter for different L/D ratio and eccentricity

Sl.No.	L/D	Eccentricity (ϵ)	Bearing Number	Sommerfeld Number	Dimensionless Bearing Force	Reference Force (N)	Bearing Force (N)	Attitude angle (degree)	Iteration completed	Relative error of pressure estimation	Absolute error of Force (N)
1	1	0.5	6.287	0.1466	1.0037	287.126	288.194	53.39	6697	9.99406E-05	0
2	0.5	0.5	6.287	0.4404	1.3364	35.89	47.9645	53.417	8126	9.99336E-05	0.11
3	0.25	0.5	6.287	1.3887	1.6954	4.486	7.6061	62.77	5061	0.003650521	1.812350981
4	1	0.4	6.287	0.2285	0.6438	287.1264	184.865	60.63	6810	9.99255E-05	0
5	0.5	0.4	6.287	0.6993	0.8415	35.89	30.21	60.73	8208	9.99606E-05	0.11
6	0.25	0.4	6.287	2.022	1.164	4.4863	5.2236	73.31	5016	0.0038	1.43
7	1	0.3	6.287	0.3573	0.4117	287.126	118.22	67.883	7056	9.99406E-05	3.04
8	0.5	0.3	6.287	1.1072	0.5315	35.89	19.0784	68.04	8308	9.99099E-05	0.11
9	0.25	0.3	6.287	2.8006	0.84064	4.4863	3.7714	84.25	5061	0.0043	0.82
10	1	0.2	6.287	0.596	0.2467	287.1265	70.89	75.245	6972	9.99871E-05	2.85
11	0.5	0.2	6.287	1.5408	0.382	35.89	13.71	80.95	5061	0.002489	7.22
12	0.25	0.2	6.287	3.305	0.71228	4.4863	3.1955	-57.17	3374	0.00097	1.72
13	1	0.1	6.287	1.2632	0.1164	287.1264	33.44	82.742	7098	9.99083E-05	0
14	0.5	0.1	6.287	3.8629	0.15237	35.8908	5.4686	83.581	7592	0.00032	2.29
15	0.25	0.1	6.287	4.4037	0.53463	4.4863	2.3985	-32.1194	3374	0.000933	2.61

8.3 Supplementary Material

Chart for determining the position of the minimum film thickness h_0. (Raimondi and Boyd.)

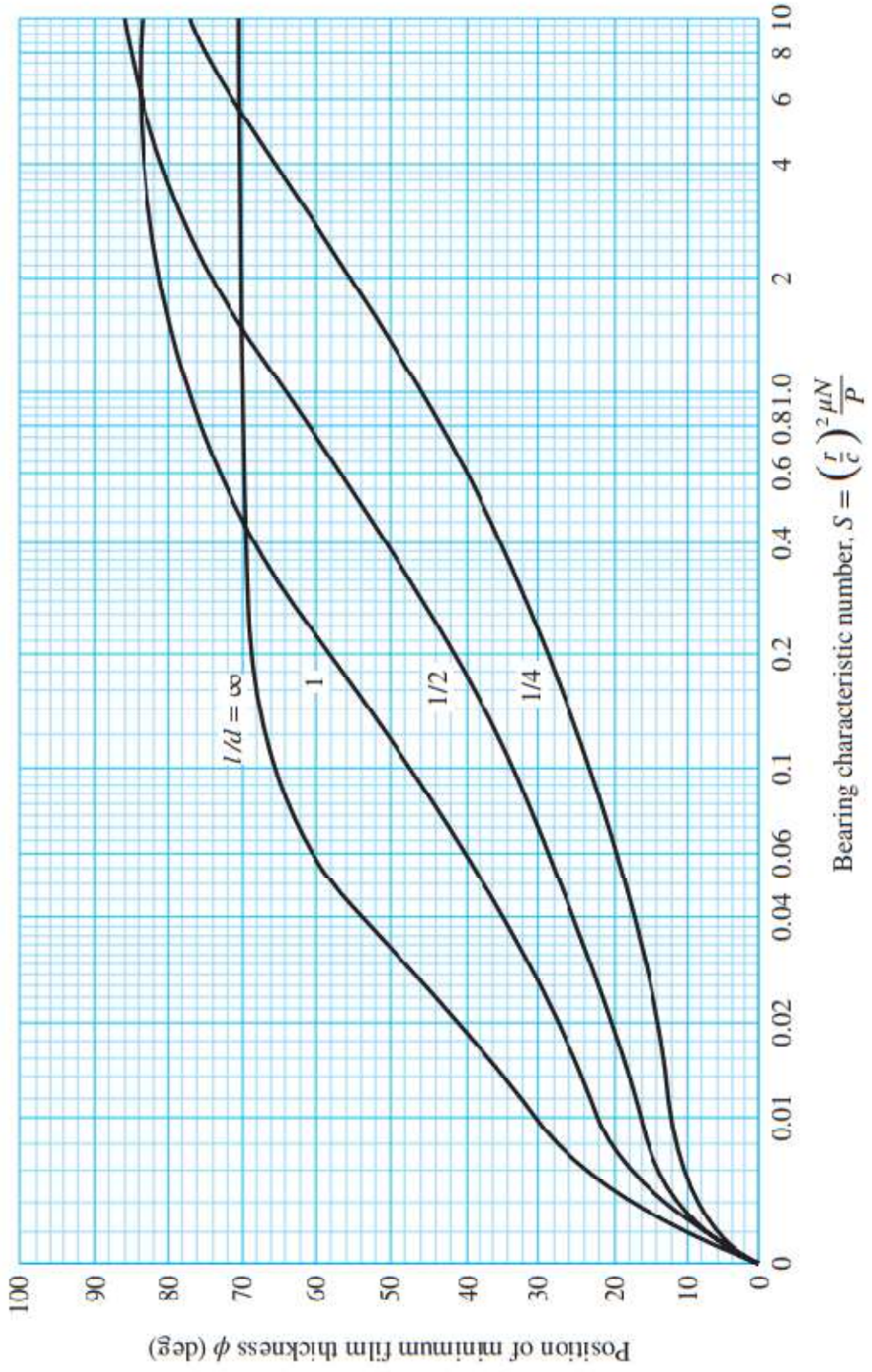

Figure 20. Chart for determining the position of the minimum film thickness h_0. (Raimondi and Boyd.)
(Source: Richard G. Budynas et al. "Shigley'S Mechanical Engineering Design (SIE)")

CORRIGENDUM

Simulation of Journal Bearings in Single cylinder Four-Stroke IC Engine: A Numerical Approach

Submitted by

ANUJ SHAW

Class Roll Number: 002211204004

Registration Number: 163718 of 2022-23

Examination Roll Number: M4AUT24003

Academic Session: 2022-2024

Under the guidance of

PROF. DR. SUSENJIT SARKAR

Department of Mechanical Engineering

Jadavpur University

188, Raja S.C. Mullick Road,

Kolkata – 700032

DECLARATION OF ORIGINALITY AND COMPLIANCE OF ACADEMIC ETHICS

I hereby declare that the thesis entitled "**SIMULATION OF JOURNAL BEARINGS IN SINGLE CYLINDER FOUR-STROKE IC ENGINE: A NUMERICAL APPROACH**" contains literature survey and original research work by the undersigned candidate, as a part of his *MASTER OF ENGINEERING IN AUTOMOBILE ENGINEERING* under the *DEPARTMENT OF MECHANICAL ENGINNERING*, studies during academic session *2022-2024.*

All information in this document have been obtained and presented in accordance with the academic rules and ethical conduct.

I also declare that, as required by these rules of conduct, I have fully cited and referenced all the material and results that are not original to this work.

Name: **ANUJ SHAW**

Class Roll Number: **002211204004**

Registration Number: **163718 of 2022-23**

Examination Roll Number: **M4AUT24003**

Date:

Signature of Candidate

FACULTY OF ENGINEERING & TECHNOLOGY

DEPARTMENT OF MECHANICAL ENGINEERING

JADAVPUR UNIVERSITY

KOLKATA

CERTIFICATE OF APPROVAL

The foregoing thesis, entitled "**Simulation of Journal Bearings in Single cylinder Four-Stroke IC Engine: A Numerical Approach**" is hereby approved as a creditable study in the area of Automobile Engineering carried out and presented by **ANUJ SHAW** in a satisfactory manner to warrant its acceptance as a prerequisite to the degree for which it has been submitted. It is notified to be understood that by this approval, the undersigned do not necessarily endorse or approve any statement made, opinion expressed and conclusion drawn therein but approve the thesis (corrigendum) only for the purpose for which it has been submitted.

Prof. Dr. Susenjit Sarkar

THESIS SUPERVISOR
Department of Mechanical Engineering
Jadavpur University, Kolkata

This corrigendum report documents the changes made to the thesis titled Simulation of Journal Bearings in A Single cylinder Four-Stroke IC Engines: A Numerical Approach " submitted on 30th Aug, 2024. Based on consultation with my supervisor, the following comments/ changes have been made:

Comment -1:

Thesis Title Change

- Original Title: Simulation of Journal Bearings in A Single cylinder Four-Stroke IC Engines: A Numerical Approach

- Comment: Minor change in thesis title without "A" before single cylinder and omitting "s" of the word "Engines".

- New Title: Simulation of Journal Bearings in Single cylinder Four-Stroke IC Engine: A Numerical Approach

Comment - 1:

Page i: Notation for phase angle (∅) in expression of Local film thickness

- Comment: Need to correct the notation for phase angle (∅)

- Correction: The notation for phase angle should be "∅" instead of "ϕ".

Thus, Correct expression for local film thickness, $h = c(1 - \varepsilon \cos(\theta - \emptyset))$ mm

Comment - 2:

Page ii: Unit of angular velocity

- Comment: There is a typographical error in the unit of angular velocity of the journal.

- Correction: The correct unit for angular velocity should be "rad/s" instead of "red/s".

Comment - 3:

Page 9: Equations (1.1) to (1.5)

- Comment: Equation numbering should be in same format throughout the report.

- Correction: The equations should be referred to as equation (1) to (5).

Comment - 4:

Page 10: Equations (1.6), (1.7) and (1.8)

- Comment: Equation numbering should be in same format throughout the report.

- Correction: The equations should be referred to as equations (6), (7) and (8).

Comment - 5:

Page 10: First paragraph, "Fig. 1.1"

- Comment: Correction in figure number in first paragraph

- Correction: Fig. 1.1 should be read as Figure 3.

Comment - 6:

Page 11: Equations (1.9), (1.10) and (1.11)

- Comment: Equation numbering should be in same format throughout the report.

- Correction: The equations should be referred to as equations (9), (10) and (11).

Comment - 7:

Page 12: Equations (1.12) and (1.13)

- Comment: Equation numbering should be in same format throughout the report.

- Correction: The equations should be referred to as equations (12) and (13).

Comment - 8:

Page 12: Last paragraph, "equation no. 1.9 & 1.10"

- Comment: Equation numbering should be in same format throughout the report. And required minor correction in equation number in last paragraph.

- Correction: The sentence "*Now putting the expression of P_p in equation no. 1.9 & 1.10*" should be read as "*Now putting the expression of P_p in equation no. 9 & 11*"

Comment - 9:

Page 13: Equations (1.14), (1.15) and (1.16)

- Comment: Equation numbering should be in same format throughout the report.

- Correction: The equations should be referred to as equations (14), (15) and (16).

Comment - 10:

Page 17: Equation (2)

- Comment: Equation numbering should be in same format throughout the report.

- Correction: The equation should be referred to as equation (17).

Comment - 11:

Page 18: Equations (3) and (4)

- Comment: Equation numbering should be in same format throughout the report.

- Correction: The equation numbers should be referred to as equations (18) and (19).

Thus, in the sentence "*Using the Finite Difference Method (FDM), equation (3) can be reformulated in a manner similar to the approach described by* ***Huang [14]****.*", equation (3) should be referred to as equation (18).

Comment - 12:

Page 18: Expression of co-efficient *F*

- Comment: There is a typographical error in the expression of co-efficient ***F***

- Correction: In the expression of co-efficient ***F***, $\dot{\emptyset}$ should be there instead of $\dot{\phi}$

Comment - 13:

Page 19: Equation (5)

- Comment: Equation numbering should be in same format throughout the report.

- Correction: The equation should be referred to as equation (20).

Thus, the sentence "*The pressure equation (4) is rewritten in the form of equation (5)*", should be read as "*The pressure equation (19) is rewritten in the form of equation (20)*".